The Recarbonation of Crushed Concrete from a New Zealand Perspective

A thesis submitted in partial fulfilment

of the requirements for the degree

of

Master of Science in Chemistry

at the

University of Canterbury

by

Kiran Dayaram

UNIVERSITY OF CANTERBURY
Te Whare Wānanga o Waitaha
CHRISTCHURCH NEW ZEALAND

February 2010

Acknowledgements

The research presented in this thesis is the culmination of two years work, and there are many people I must express my gratitude to.

Firstly I must thank my supervisor at the University of Canterbury, Dr Paul Kruger, for this support, guidance, courage to supervise a thesis outside his immediate area of expertise and last minute revisions of this thesis. His problem solving abilities and open door policy really aided in the completion of this research.

Secondly I must thank my supervisors at Holcim (NZ) Ltd, Greg Slaughter and Michael Rynne for their financial and technical support. There knowledge and ability to keep my work in perspective was very valuable.

To the technical staff in the Chemistry Department at the Univeristy of Canterbury who have been indispensable:

Thanks to:

- Steven Graham for helping to fix, design and build all things electrical.
- Wayne MacKay for helping construct and fix all things mechanical.
- Robert McGregor for modifications to the glass desiccators.
- John Davis for the help with sourcing a new computer and dealing with network problems and printers.

Thanks must also go to the following people from the Engineering Department at the University of Canterbury:

- James MacKechnie for the supply of New Zealand mix designs and teaching me about concrete preparation.
- Tim Perigo for helping me to cast the concrete test cyinders and allowing me the use of the facilities in the concrete laboratory.
- Julian Murphy for help with the programming of LabView and ability to make any electrical circuit work.

Lastly I must thank my family who have been ever supportive of me and my studies. To my Mum and Dad thank you for your guidance and support both financial and emotional. Without you this thesis would not be what it is today. To my brother and sister thank you for helping me when I have been busy and irritated and taking it all in your stride, I will never forget the support you have given me.

Abstract

The cement industry releases large quantities of CO_2 into the atmosphere during the manufacture of Portland Cement. The intrinsic property of the cement to reabsorb some of this CO_2 over its life time through a process called recarbonation has been investigated. This thesis reports on the development of an accelerated recarbonation apparatus for studying the recarbonation of crushed concrete under controlled conditions.

The apparatus involved a series of airtight desiccators into which were placed the crushed concrete samples. The desiccators were then filled to ~50,000 ppm CO_2, which is significantly greater than the ~380 ppm by volume CO_2 available in the earth's atmosphere. The CO_2 concentration was then monitored with respect to time inside the desiccator using CO_2 specific infrared probes. Two concrete design strengths of 20MPa and 40MPa with various crushed particle sizes were exposed to conditions of 50-60 % relative humidity, a temperature of 20 ± 1.5 °C, an exposure period of 21 days and a maximum CO_2 concentration of ~50,000 ppm by volume. The CO_2 uptake measured by the infrared probes was verified using other detection methods of FTIR, TGA, XRF, phenolphthalein indicator and the weight gain of the crushed concrete samples.

The research found that a concrete of 20 MPa design strength and a water to cement ratio of 0.67 could absorb 12-83 % of the original calcination emissions for particle sizes <40, <20 and <10 mm in the 21 day time period. Similar behaviour was also exhibited by the 40 MPa design strength (w/c 0.49) but the extent of CO_2 uptake was not as pronounced. The 40 MPa (w/c 0.49) design mix absorbed 9-70 % of the original calcination emissions for the same particle sizes of <40, <20 and <10 mm. It was found that significant quantities of CO_2 could be absorbed by the smaller crushed sizes of <10 and <20 mm for both design mixes, owing to their much larger surface area. It was also found that about 80 % of the total CO_2 absorbed occurred within the first 10 days of exposure.

It is envisaged that the results contained in this thesis will assist in future investigations into crushed concrete recarbonation.

Table of Contents

Abbreviations

CS	Calcium silicates
CSH	Calcium silicate hydrates
C_3S	Tricalcium silicate
C_2S	Dicalcium silicate
C_3A	Tricalcium aluminate
C_4AF	Tetracalcium aluminoferrite
FTIR	Fourier transform infrared
IR	Infrared
TGA	Thermal gravimetric analysis
XRD	X-Ray Diffraction
OPC	Ordinary Portland Cement
XRF	X-Ray Fluorescence
w/c	Water to Cement Ratio

1.0 Introduction

1.1 Cement and its Environmental Impact

Cement is the most widely used man made product in the world [1]. Global cement production is estimated at 2.77×10^9 tonnes annually. The environmental carbon dioxide load from this production is estimated at 2.4×10^9 tonnes [2]. Fifty percent of the carbon dioxide produced during manufacture is due to fossil fuel consumption. The other fifty percent is due to the calcination of the limestone [3]. The carbon dioxide produced in the calcination process may be mitigated by recarbonation of concrete. The study of this process is the basis of this thesis.

Climate change and its affect on the environment are becoming important and often contentious issues. In this context it is vital that the cement and concrete industry recognize its impact on the environment and the various ways in which it may be able to negate the detrimental impacts.

Many studies carried out in the last 50 years have dealt with concrete carbonation. However, most of this research has been directed at minimizing carbonation in concrete structures. The Holy Grail for engineers has been to design concrete structures that do not undergo carbonation, as it can lead to structural failure. Carbonation of concrete causes a drop in the pH and promotes the degradation of the electrochemical protection of the steel reinforcement resulting in corrosion and structural failure [4].

Current research in concrete carbonation is now being directed at the beneficial effects of this process in the way that it reduces the carbon dioxide load in the atmosphere. This thesis is an extension of that research.

Carbonation and recarbonation are identical processes that occur in concrete that involve the absorption of carbon dioxide from the atmosphere. Carbonation is a slow process associated with intact concrete structures. Recarbonation is a much more accelerated process that occurs in crushed and demolished concrete. This thesis examines the carbon dioxide absorption of crushed and demolished concrete made with Ordinary Portland Cement (OPC).

Cement manufacture varies throughout the world depending on the raw materials available and manufacturing process used. In New Zealand both the wet and dry processes are used in the manufacture of cement. The dry process is a more energy efficient way of producing cement as the raw materials are blended together while dry before entering the kiln. In a wet process plant the raw materials are blended with water to create a slurry before entering the kiln. Water has to be driven off from the slurry and this process is energy intensive, requiring on average 2400 kJ more energy than a dry process would for the production of one kilogram of clinker [5]. On average in New Zealand 850 kg of carbon dioxide is released during the manufacture of every tonne of cement [6,7].

1.2 Manufacture of New Zealand Ordinary Portland Cement

New Zealand OPC is made from limestone and marl. These two constituents are blended together and enter the cement kiln. The kiln is a long metal cylinder that is set at a slight incline and is fired by pulverized coal and recycled mineral oil [9]. As the raw mix moves down the kiln it is exposed to a temperature of 1450 ºC [6]. The raw mix becomes homogenous and creates little sintered lumps called clinker. The clinker is then ground in the milling plant and after this additives such as gypsum, limestone and blast furnace slag can be added to create cement with a specific characteristic required by the customer.

The CO_2 released during cement manufacture comes from three sources in a wet process cement plant. The first source is the burning of fossil fuels to heat the kilns and accounts for approximately forty eight percent. The second is from the calcination of limestone and accounts for forty seven percent. The other five percent is from the electricity used to run electrical equipment in the manufacturing plant such as the clinker grinding equipment. Figure 1.1 below gives a summary of the CO_2 sources.

	Contribution (%)	*Source*
Calcination CO_2	47%	Calcination of limestone raw material.
Thermal (Fuel) CO_2	48%	Combustion of fuels in wet kilns.
Electricity CO_2	5%	Combustion of fuels in generation.
Total CO_2 Emitted	100.00%	

Figure 1.1 Origins of CO_2 emissions during cement manufacture for a wet process plant, represented as a percent of total CO_2 emitted [7].

1.3 Chemistry of Cement and Concrete

1.3.1 Cement

Understanding the chemistry of the recarbonation reaction in concrete is very important to appreciate where recarbonation fits into cement's lifecycle. Previous research into the chemistry of cement, concrete and recarbonation have given great insight into the reactions that occur and the different reactants and products that are involved [3-6,10-16]. The following sections aim to give a concise description of cement, concrete and recarbonation chemistry.

Cement acts as the binding agent when mixed with water to hold sand and aggregate together in concrete. The chemistry of cement can be very complex. Before the raw materials enter the kilns, the chemistry of the major constituents can be tightly controlled. However, once in the kiln, there are multiple variables that can affect the chemistry of the clinker produced. Because of this cement chemists focus primarily on the important oxides contained within the clinker that give cement its binding properties.

Cement clinker comprises four main metal oxides that are CaO (C), SiO_2 (S), Al_2O_3 (A) and Fe_2O_3 (F), and these are responsible for the bulk of OPC. Additions to cement clinker of substances such as gypsum, limestone, blast furnace slag, fly ash and silica fume can be used to influence the properties and setting time of the desired concrete by influencing

its major constituent phases. Portland cement clinker commonly contains four major phases. These consist of alite, belite, aluminate and ferrite.

Alite constitutes the largest and most important part of the clinker accounting for 50-70 %. It is primarily comprised of tricalcium silicate (Ca_3SiO_5) or C_3S and is the most important phase in strength development up to 28 days. Belite makes up 15-30 % of the cement clinker mass and is dicalcium silicate (Ca_2SiO_4) or C_2S. This phase is important in later strength development, typically after 28 days, as it reacts slowly with water. Aluminate ranges between 5-10 % in Portland cement clinker and is tricalcium aluminate ($Ca_3Al_2O_6$) or C_3A. This phase reacts very quickly with water and can cause very fast setting. A controlling agent, most commonly gypsum is added to regulate the setting of the aluminate phase. The fourth major phase is Ferrite, which is tetracalcium aluminoferrite (Ca_2AlFeO_5) or C_4AF and constitutes 5-15 % of the cement clinker. It typically reacts with water quite rapidly but this can be rather variable due to the ratio of Fe and Al present in the phase. All the above compounds can be modified in composition and crystal structure by ionic substitutions [5].

The hydration of the calcium silicates is mainly responsible for the cementing properties of Portland cement and the production of the compounds involved in recarbonation.

1.3.2 Concrete and Cement Hydration

Concrete is a mixture of cement, water, sand and aggregate. The cement acts as a glue to bind the sand and aggregate together. Different concrete strengths are achieved by changing the proportions of the above ingredients. Special concrete applications can have other materials added, called plasticizers, which alter the concrete characteristics. The hydration of cement refers to the anhydrous cement being mixed with water. Gypsum, a calcium sulfate ($CaSO_4$) containing material, is blended with the Portland Cement to help control the setting rate and the strength development. Although it is only added in small proportions (0-5%) it plays an important role in the cement chemistry [6]. The reactions involved are more complex than the simple conversion of anhydrous compounds to their respective hydrates, with full hydration taking a long time to achieve. Cement chemistry reactions are therefore written as sums of their oxide composition.

The hydration of the calcium silicate phases are the most important reactions in relation to concrete strength development and yields nearly amorphous calcium silicate hydrate (C-S-H) and calcium hydroxide ($Ca(OH)_2$), as shown in equations **(1)** and **(2)** [6]. It is these two compounds that play an important role in the recarbonation process. C-S-H is a generic name for any amorphous or poorly crystalline calcium silicate hydrate [22].

Hydration of Calcium Silicates:

$$2(3CaO.SiO_2) + 6H_2O \bullet \quad (3CaO.SiO_2.3H_2O) + 3Ca(OH)_2 \qquad \textbf{(1)}$$

$$2(2CaO.SiO_2) + 4H_2O \bullet \quad (3CaO.SiO_2.3H_2O) + Ca(OH)_2 \qquad \textbf{(2)}$$

The C_3A component of the cement clinker goes through two stages during hydration. This reaction is very rapid and the addition of gypsum ($CaSO_4$) is used to control the rate of this reaction. The first stage is the conversion of C_3A to high-sulfate calcium sulfatealuminate. This product will endure until all the sulfate has been consumed from the pore solution. The second stage is the hydration of high-sulfate tetracalcium sulfoaluminate to produce low-sulfate tetracalcium sulfatealuminate (C_4AH_{13}) [5,6,22]. These reactions are represented in equations **(3)** - **(5)**.

Hydration of Tricalcium Aluminate:

$$(3CaO.Al_2O_3) + 3(CaSO_4) + 26H_2O \bullet \quad (6CaO.Al_2O_3.3SO_3.32H_2O) \qquad \textbf{(3)}$$

$$2(3CaO.Al_2O_3) + (6CaO.Al_2O_3.3SiO_2.32H_2O) + 4H_2O \bullet$$

$$3(4CaO.Al_2O_3.SO_3.12H_2O) \qquad \textbf{(4)}$$

$$(3CaO.Al_2O_3) + Ca(OH)_2 + 12H_2O \bullet \quad (4CaO.Al_2O_3.13H_2O) \qquad \textbf{(5)}$$

The hydration of C_4AF has been the hardest to study as it forms very few stable structures. It combines initially with gypsum and lime to form high-sulfate sulfoaluminate and sulfoferrite. Once all the sulfate has been consumed it undergoes a similar transition

to C_3A and transforms into the low-sulfate aluminoferrite solid solution and a more intricate solid solution phase where the sulfate ion is replaced by a hydroxyl ion. Both the hydration of aluminate and ferrite has been shown to be retarded by both gypsum and $Ca(OH)_2$ [5,6].

1.4 Recarbonation Theory and Chemistry

The chemistry of concrete recarbonation is simple in theory but very complex in practice and it varies around the world according to the use of different raw materials and additives.

The first important reactions involve the hydration of the cement during the mixing and curing of the concrete, the major components of which are tricalcium silicate ($3CaO.SiO_2$), dicalcium silicate ($2CaO.SiO_2$), tricalcium aluminate ($3CaO.Al_2O_3$), tetracalcium aluminoferrite ($4CaO.Al_2O_3.Fe_2O_3$) and gypsum ($CaSO_4$). Of these, the calcium silicates are the most important in relation to concrete recarbonation. Upon addition of water during the mixing, the calcium silicates form calcium silicate hydrates (CSH) and calcium hydroxide [3,16-24,40]. These two compounds are responsible for the majority of the carbon dioxide uptake during recarbonation.

The equations below represent the major species involved during recarbonation:

<u>Recarbonation:</u>

$$Ca(OH)_2 + CO_2 \bullet \quad CaCO_3 + H_2O \qquad \textbf{(6)}$$

$$(3CaO.SiO_2.3H_2O) + 3CO_2 \bullet \quad (3CaCO_3.2SiO_2.3H_2O) \qquad \textbf{(7)}$$

$$(2CaO.SiO_2) + 2CO_2 + nH_2O \bullet \quad (SiO_2.nH_2O) + 2CaCO_3 \qquad \textbf{(8)}$$

$$(3CaO.SiO_2) + 2CO_2 + nH_2O \bullet \quad (SiO_2.nH_2O) + 3CaCO_3 \qquad \textbf{(9)}$$

The recarbonation reaction is diffusion controlled, as the carbon dioxide has to diffuse into the solid concrete matrix to react with the hydrated species present in the concrete [11-13]. The strongest recarbonation reaction is that of $Ca(OH)_2$, followed by CSH, and then the calcium silicates whose rates are very similar. It takes a long time for full hydration to be achieved [6].

The calcium silicate hydrates exist in at least five different morphologies as seen in previous research [3,5,6,11-13]. The exact species present in the concrete are of little importance for this research as they all exhibit recarbonation chemistry.

In order for the carbon dioxide to react with the species in the concrete matrix it must first undergo hydration to give carbonic acid. The carbonic acid can then dissociate into its ionic states of carbonate (CO_3^{2-}) and bicarbonate (HCO_3^{2-}) ions, represented in equations **(10)**, **(11)** and **(12)**. The amount of carbonate ion that is formed is determined by the pH of the concrete. At a high pH (above pH 10), the carbonate ion is dominant. At a lower pH (below pH 10), the bicarbonate ion is the dominant ion.

$$CO_{2(g)} + H_2O \bullet \quad H_2CO_3 \qquad \textbf{(10)}$$

$$H_2CO_3 + H_2O \bullet \quad HCO_3^- + H_3O^+ \qquad \textbf{(11)}$$

$$HCO_3^- + H_2O \bullet \quad CO_3^{2-} + H_3O^+ \qquad \textbf{(12)}$$

The first species consumed in the recarbonation process is the calcium hydroxide equation **(6)**. Once most of the calcium hydroxide is consumed the calcium silicate hydrates will then undergo recarbonation releasing calcium ions. The release of calcium ions from the calcium silicate hydrates will then form more calcium hydroxide that will then undergo recarbonation. Once recarbonated, the calcium silicate hydrates yield calcium carbonate and silica gel. As the pH drops below 11, the other species present in the concrete matrix that contain CaO such as the hydrated products of aluminate and ferrite will also undergo recarbonation [3,5]. Since these species are present in much smaller quantities, their influence on CO_2 uptake is much less than that of calcium silicate hydrates.

1.5 Environmental Influences on Recarbonation

Variables such as humidity, porosity, water/cement ratio, addition during blending of pozzolanic materials, environment, strength and temperature determine the rates of the above reactions [3,5,6,10-22].

Humidity plays an important role in concrete recarbonation. If the concrete is too wet, then the carbon dioxide will dissociate in the surface water thus preventing penetration into the concrete pores that enables recarbonation inside the concrete. The opposite applies also: if the concrete is too dry, the diffusion is fast but the recarbonation is slow due to a lack of water for the hydration of carbon dioxide. The optimum relative humidity for recarbonation is in the range of 50-75 % [5,6,20-22].

Concrete porosity strongly influences recarbonation rate. As porosity increases, carbon dioxide diffusion increases resulting in an increased recarbonation rate. Porosity is controlled by the water/cement ratio. A low water/cement ratio will decrease the porosity and a high water/cement ratio will increase the porosity [13]. Concrete strength and density is inversely proportional to porosity. The denser the concrete becomes the slower the recarbonation rate as the concrete matrix becomes more confined. Concrete products such as masonry blocks will generally recarbonate faster than conventional concretes because they are lower strength and therefore more porous.

Pozzolanic materials are used as supplementary cementitious materials. Pozzolans when combined with calcium hydroxide exhibit cementitious properties and commonly comprise of vitreous siliceous materials. Pozzolanic materials in concrete increase the recarbonation rate because there is less cement used in the concrete itself [15]. The lowering of the cement content means that less calcium oxide is present to undergo recarbonation, therefore, the relative rate should increase as the smaller concentration of calcium oxides present will recarbonate quickly.

The environment has a big impact on the recarbonation rate. Indoor conditions are found to be more favorable for recarbonation owing to the higher humidity and temperatures. Concrete on the interior of buildings will also recarbonate faster than exterior concrete due to the presence of more CO_2 expelled by the human occupants. Buried concrete will

recarbonate albeit at a slow rate as the carbon dioxide will have to diffuse through the soil. It has been argued by Engelsen et al. 2005 [10], that degradation of organic matter in the ground will increase the amount of carbon dioxide. But the interaction of this with the concrete is as yet unknown. Coating concrete in paint or a sealant will also slow the recarbonation rate.

1.6 Thesis Rationale and Objectives

The above sections have described how concrete both crushed and *in-situ* undergoes recarbonation and carbonation respectively. The carbonation of *in-situ* concrete has been well documented in the past. The recarbonation of crushed and demolished concrete has only begun to be investigated in Europe and North America.

In a New Zealand context very few research articles are available on the effect of recarbonation on crushed and demolished concrete. The overall aim of this research is to determine the extent of CO_2 absorption by crushed concrete made with Ordinary Portland Cement.

The physical testing of the concrete specimens was carried out in the Civil Engineering Department at the University of Canterbury and the recarbonation testing was done in the Chemistry Department at the University of Canterbury.

Specific objectives were as follows:

1. Develop a test setup to measure the uptake of carbon dioxide by crushed concrete.
2. Determine how much carbon dioxide could be absorbed by crushed concrete and its potential value for CO_2 reductions.
3. Determine how concrete composition and crushed concrete size affect the uptake of carbon dioxide by crushed concrete.

2.0 Sample Preparation and Experimental Setup

2.1 Sample Preparation and Physical Testing

Cement comes in many different varieties depending on their specific use. Different varieties are made by blending additives with the cement. These additives can include gypsum, blast furnace slag, fly ash, silica fume and limestone. Ordinary Portland Cement (OPC) is the most commonly used cement in New Zealand and the world. The additives contained in New Zealand OPC are gypsum and limestone. The thesis addresses the recarbonation of OPC because it is the most popular and widely used variety.

The water to cement ratio (w/c) of concrete has been shown to influence the recarbonation rate. This is also the key influence on strength development both late and early in the concrete [4,5,6]. Two design strengths were identified for the recarbonation testing. These were standard 20 MPa and 40 MPa design mixes using OPC. Each has a water to cement ratio of 0.67 and 0.49, respectively. Dr James MacKechnie from the Civil Engineering Department at the University of Canterbury supplied the design mixes based on what was used commercially in New Zealand. 20 MPa and 40 MPa design mixes were used as they represent the most common concrete strengths used in New Zealand. Details of the designs used and physical properties are contained in Tables 2.1 and 2.2.

Concrete Mix Designs 50L		
Ingredients	**20MPa**	**40MPa**
Water (L)	8	8.5
Cement (kg)	12	17.235
13mm Aggregate (kg)	52.5	56
Sand (kg)	42.5	40
Air Entrainer (mL)	5	5
Water Reducer (mL)	50	50
7 Day Strength (MPa)	28.3	37.6
14 Day Strength (MPa)	29.8	39.7
28 Day Strength (MPa)	31.7	40.5
Density (g.cm-3)	2.35	2.38

Table 2.1 Concrete design mixes used in sample preparation and the physical characteristics of the concrete cylinders.

The concrete samples to be tested needed to be uniform and meet all relevant New Zealand standards to ensure reproducibility and guarantee that the concrete samples would be representative of concrete used in the real world. All concrete test cylinders were produced according to New Zealand Standard 3112-1986 [37].

Commercial jaw crushers are used to crush concrete to a predetermined size. Crushing of the concrete samples was originally planned to be done in a variable jaw crusher. This was to be a problem as a variable crusher with the specific characteristics needed was unable to be sourced in Christchurch. Therefore it was decided to crush the samples manually using a compressive strength machine and screen the sample through a sieve to attain the appropriate size. Any particles that could not pass through the sieves were recrushed either in the compressive strength machine or manually using a hammer and chisel.

The particle size of the crushed concrete was controlled. Particle sizes of <10 mm, <20 mm, <40 mm and uncrushed were selected for testing. The first two sizes of <10 mm and <20 mm were used as these sizes have been used successfully in recycling projects such

as aggregate for the production of more concrete and sub-base fill [35,36]. The <40 mm sample was tested to see the effect of recarbonation on larger particles of crushed concrete and how particle size contributed to carbon dioxide uptake. The uncrushed samples were sections of the cast cylinders that were used as controls to show the recarbonation extent if the concrete was not crushed. This would help to identify the rate differences between crushed and uncrushed concrete.

Particle size distributions were obtained for the samples to show that they were representative of the stated particle sizes. The particle size distribution measurement was obtained by passing 500 g of the crushed concrete through a series of sieves with decreasing apertures. The fractions left on each sieve could then be used to calculate what percentage of the total was retained. The sieves used were obtained from the Geology Department at the University of Canterbury. The apertures used were 32 mm, 16 mm, 8 mm, 4 mm, 1 mm and 250 µm. The results for the particle size distributions are summarised in Table 2.2 and Figures 2.1 and 2.2.

Concrete Strength	**Average Percentage Retained on Sieve of 500g Crushed Concrete Fraction**						
	32 mm	**16 mm**	**8 mm**	**4 mm**	**1 mm**	**250 µm**	**<250 µm**
20 MPa							
<10 mm			39	31	24	4	2
<20 mm		39	37	14	7	2	1
<40 mm	42	38	17	2.5	0.5		
40 MPa							
<10 mm			38	32	22	6	2
<20 mm		37	39	12	8	3	1
<40 mm	40	40	15	3	1.5	0.5	

Table 2.2 Particle size distributions for 20 MPa and 40 MPa samples given as a percentage retained on a sieve of specific grading size.

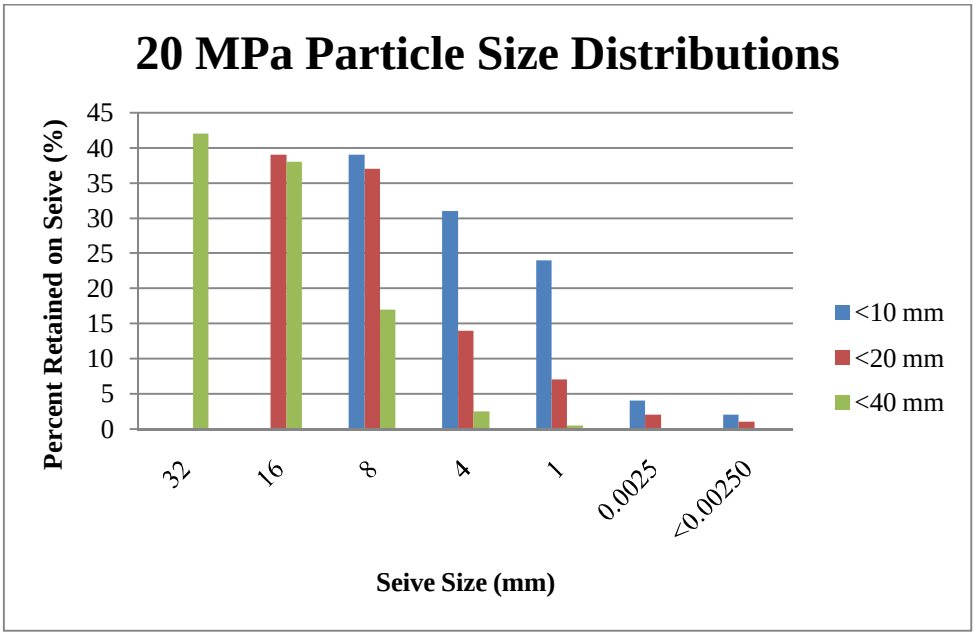

Figure 2.1 20 MPa particle size distributions for <10 mm, <20 mm and <40 mm samples prior to testing.

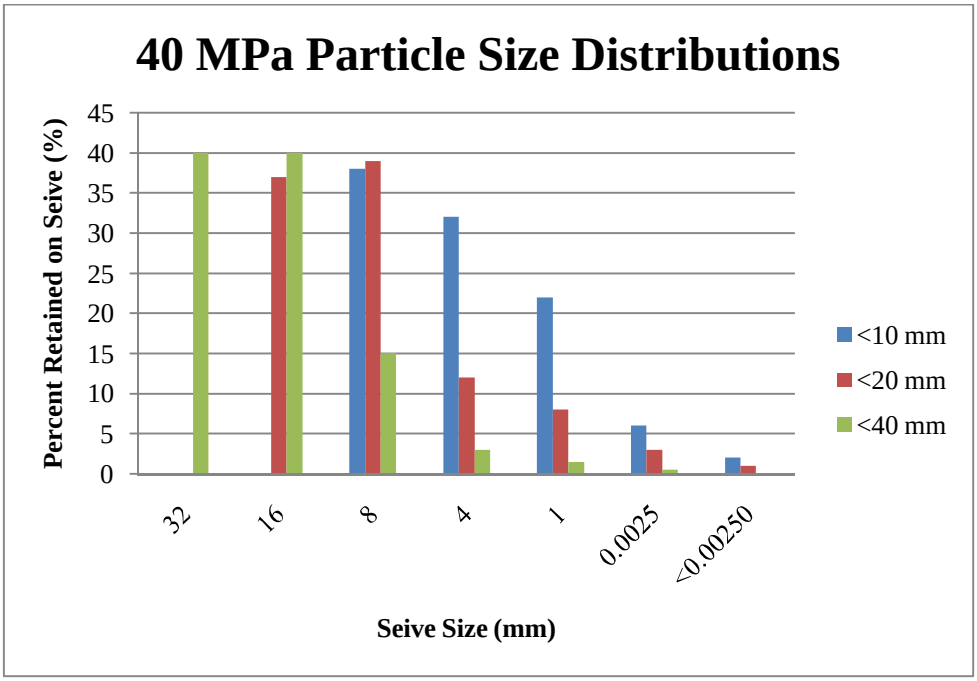

Figure 2.2 40 MPa particle size distributions for <10 mm, <20 mm and <40 mm samples prior to testing.

The reproducibility of results is paramount in any scientific investigation. This involved making sure that the same materials and conditions were used for the preparation and curing of the concrete samples. The cement used was Holcim Ultracem which is Holcim's OPC. The sand and aggregate was sourced locally so as to eliminate any variation in the concrete chemistry. If at any point the samples were exposed to the atmosphere then it was important that all samples be exposed for exactly the same time as to reduce the influence of any recarbonation that may take place prior to testing.

The preparation of the samples took place in the Concrete Laboratory in the Civil Engineering Department at the University of Canterbury. The concrete was prepared in 50 L batches to ensure that 20 test cylinders could be cast for each batch. Each cylinder was 200 mm high and 100 mm in diameter. The recipes for the concrete batches as described in Table 2.1 were cast into 20 steel moulds and demoulded the following day. A small quantity of air entraining agent was used to increase the workability of the concrete. Water reducer was also used to increase workability and reduce the amount of water and cement used while allowing the same design strength. They were then placed in a 100 % relative humidity fog room to cure for 28 days. Compressive strength measurements were taken on an Avery Model 711 CC6 compressive strength machine at 7, 14 and 28 days to ensure the cylinders were curing correctly and the design strengths were being achieved. Density measurements were also taken at 28 days to ensure the density of the concrete samples was correct and is shown in Table 2.1. After 28 days the samples were immediately placed inside the storage containers. The samples were then kept in these jars for three months before testing on them commenced to allow greater hydration of the concrete cylinders to take place. XRF analysis (Table 2.3) of the cement used in each batch was also performed so that the effective oxide weight percentages of the important elements could be determined, and theoretical uptakes could be established to ensure the cement was the correct quality.

	Oxide Weight %								
Holcim Ultracem	CaO	SiO_2	Al_2O_3	Fe_2O_3	SO_3	MgO	K_2O	Mn_2O_3	Loss
20MPa	63.8	20	4.2	2.2	2.8	0.7	0.7	0.2	5.4
40MPa	64.1	20.1	4	2.1	2.7	0.7	0.7	0.2	5.4

Table 2.3 XRF analysis of Holcim Ultracem cement used in sample preparation.

2.2 Sample Storage

Storage of the samples prior to testing was also a challenge that needed to be addressed. Various containers were considered for sample storage. The requirements were that they needed to exclude carbon dioxide and water so that negligible recarbonation would take place before testing began. Airtight containers made of polyvinyl chloride (PVC) and polystyrene (PS), were tested for their storage suitability. Polyethylene terephthalate (PET) was also considered for storage as it is used in Coca Cola bottles to stop carbon dioxide permeation. PET was not a viable option due to the limited size range of the containers available. PS and PVC were also the most cost effective containers, as at least fifteen containers would be needed to store the samples.

Figure 2.3 Click Clack container with concrete sample inside.

Testing of the storage containers was done by placing 1 L of 2 mol. L^{-1} calcium hydroxide solution in each container and then sealing them. A container open to the atmosphere was also used as a control to show what happens if atmospheric carbon dioxide is able to react with the calcium hydroxide solution. The suitability of each would be determined by monitoring the pH of the solution in each container with universal litmus paper over a period of three months. If any of the solutions were exposed to carbon dioxide the calcium hydroxide would react with the carbon dioxide to produce a milky solution of calcium carbonate and the pH of the solution would be lowered.

After one week the control solution had become cloudy with the presence of calcium carbonate. This showed the calcium hydroxide solution had reacted with atmospheric carbon dioxide. The pH of the control solution was still ~12 and the sealed containers were still colourless and a pH of ~14. After one month the control solution had become very cloudy and the pH had dropped to ~7. The containers that were sealed were still exhibiting a pH of 12-14 and were still colourless. The PVC container had a slightly lower pH than the polystyrene container. After three months the control solution was at a pH ~6 and the PVC and polystyrene containers were at a pH ~12 and pH ~13

respectively. The above results support the use of polystyrene containers for sample storage as they exhibited the best resistance to carbon dioxide permeation. The fifteen containers were Click Clack polystyrene airtight containers (see Fig 2.3) and were purchased from Pay Less Plastics in Christchurch.

2.3 Previous Accelerated Carbonation Studies

Most previous accelerated carbonation studies have dealt with the carbonation of *in-situ* concrete samples [11-16]. Few have dealt with crushed concrete recarbonation. Accelerated carbonation studies are used to investigate carbon dioxide absorption. This is because the carbonation reaction is very slow under normal atmospheric carbon dioxide concentrations. Acceleration studies are carried out by increasing the carbon dioxide concentration exposure of the concrete while simultaneously controlling exposure conditions such as temperature and humidity. The following reviews of past papers encompass accelerated carbonation studies and recarbonation detection methods such as phenolphthalein, fourier transform infrared spectroscopy (FTIR), X-Ray diffraction (XRD) and thermal gravimetric analysis (TGA).

A recent study by Engelsen *et al*. 2005 [10] has looked specifically at the recarbonation of crushed and demolished concrete. This study was part of a wide investigation by the Nordic Innovation Centre into the carbon dioxide uptake during the life cycle of concrete. They looked at the recarbonation of crushed concrete for particle sizes 1-16 mm in controlled conditions of 5-15 % carbon dioxide over a period of 25-35 days. They looked at a range of different cements and water cement ratios ranging from 0.4-0.75.

Their experimental setup involved three airtight desiccators that had carbon dioxide specific infrared probes mounted in them. Into these they placed the crushed concrete samples and then filled them with carbon dioxide and monitored the uptake using the probes. The setup used in this experiment was fully automated using a computer programme written in Visual Basic. The probe results were verified by weighing the samples before and after carbon dioxide exposure and by IR spectrometry.

They found that 50-60 % and 60-90 % recarbonation of total CaO for concrete samples with middle and high w/c respectively. This corresponded to an uptake of 60-80 % of the

calcination emissions. As expected they also found that the lower the w/c ratio the slower the recarbonation rate.

This study was to be the basis for this thesis as it encompassed an automated and real time monitoring method. Automation is desirable as the recarbonation reaction is slow and can take a long time to complete. This point is further enforced later in the thesis during construction of the setup as manual filling of the desiccators had been tested for its suitability.

Other accelerated carbonation studies by Roy *et al*. 1998 [25] and Jerga 2004 [23] have looked at the physico-mechanical properties of carbonated concrete and the effect of humidity, concrete grade and pore size on concrete carbonation. There are numerous other studies that have investigated concrete carbonation but have been omitted in the review as they gave little details on the carbonation apparatus used. Both studies reviewed here used hermetic chambers that had a constant flow of carbon dioxide at a predetermined level, 6 % and 15 % respectively. In the study by Jerga 2004 an increased pressure was also used to increase the carbonation rate. Roy *et al*. 1998 found that humidity, concrete grade and pore size had large influences on the recarbonation rate. Relationships were drawn between concrete strengths and its effect on carbonation depth. A range of relative humidities were also tested to find the optimum range for carbonation to occur. This was found to be in the range of 55-65 % and it could be achieved using magnesium nitrate as the relative humidity control agent. It also gave insights into the role that temperature plays in influencing carbonation rates. The above studies were concerned with concrete carbonation and did not look at the effect of recarbonation on crushed concrete.

Four methods have been identified for detection of carbon dioxide and the recarbonation compounds. These are the phenolphthalein test, FTIR, TGA and powder XRD.

The easiest and cheapest method is the phenolphthalein test as described by Lo *et al*. 2001 [30]. A phenolphthalein solution was sprayed onto freshly broken concrete. Where carbonation had occurred the indictor turned pink as the pH value was low. The indicator remained colourless on uncarbonated areas of the concrete. This method gave quick identification of the carbonation front and is useful to determine carbon dioxide penetration of crushed concrete particles. Fourier-transform infrared spectroscopy was the other method employed for carbonation detection. The C-O bonds in the carbonation

product of calcium carbonate exhibit a characteristic peak in the wave number range of 1410-1510 cm^{-1}. This is the most easily identifiable peak as the complex nature of the concrete material can give many characteristic peaks for different compounds present in the concrete matrix. FTIR was also used in a number of other studies [30,32,34] as it is an easy and cheap test to carry out and requires little sample preparation and the results are easy to interpret. This method was employed in the current study to show the presence of the carbonate ion and verify that recarbonation had taken place by an increase in absorbance of the corresponding peak.

TGA and powder XRD have also been employed in past studies for detection of carbonation products. Villian *et al*. 2007 [31] used thermal gravimetric analysis and gammadensimetry for detection of calcium carbonate. Gammadensimetry is a non-destructive test that uses the absorption of gamma-rays to detect CO_2. This method can detect CO_2 both in the cement paste and the CO_2 that has reacted to form $CaCO_3$. This method was not used as the University of Canterbury did not possess a gammadensimetry apparatus and there were other methods that were more readily available for testing such as thermal gravimetric analysis (TGA). TGA has been reported in a number of studies [32,33] as an effective tool in identifying $CaCO_3$. TGA continuously measures the mass of a sample as it exposed to a temperature ramp of typically 1-2 ºC/min for a given temperature range. TGA was used for this study as there was a TGA instrument available and the analysis using this instrument is straightforward and can be done without the need of a technician or specialised conditions. The temperature at which calcium carbonate is lost is stated to be 530-900 ºC. The Villian *et al*. 2007 study also coupled the TGA with chemical analysis so that the origin of the calcium carbonates could be identified as they were using calcareous aggregates in their concrete preparation and this contributed to the $CaCO_3$ present.

A study by Chang *et al*. 2004 [32] reported similar TGA and FTIR findings for concrete carbonation. They also employed the use of powder XRD. Powder XRD is a very effective method to quantify $CaCO_3$ and $Ca(OH)_2$. Many other studies [5,6,32] have also reported similar findings using powder XRD. Powder XRD was to be employed in the production of this thesis if time allowed but delays in starting the testing and XRD diffractometer availability led to this method being abandoned.

2.4 Experimental Design and Construction

The experimental setup used for this thesis was based on a study by Engelsen *et al*. 2005 [10] for the Nordic Innovation Centre. As mentioned in the previous section their setup involved a series of airtight desiccators where CO_2 absorption could be monitored using CO_2 specific infrared probes. The ability to have real time monitoring and control of the humidity and CO_2 exposure were desirable in the test setup due to the long time each test would take and the many variables that needed to be controlled. The method used in this thesis was an adaptation of that particular setup.

The location of the testing was in Room 539 of the Chemistry Building at the University of Canterbury. The room used was air conditioned and maintained an average temperature of 20±1.5ºC. A constant temperature is required as any variance in temperature would mean variance in the recarbonation rate [3,5,6].

The humidity also needed to be controlled as it has a significant effect on the recarbonation rate. If the humidity is either too low or too high the recarbonation rate will be reduced. The optimum range is 50-75% [5,6,20-22]. Engelsen *et al*. 2005 used saturated magnesium nitrate solution as it kept the relative humidity at 50-60%. Magnesium nitrate would also be used in this study to achieve similar relative humidity conditions.

The average concentration of CO_2 in the Earth's atmosphere is ~380 ppm or 0.038% by volume [3]. An artificial CO_2 atmosphere of concentration 5% was used to accelerate the recarbonation of the concrete. This was almost 150 times the normal atmospheric concentration. The desiccators would be filled to 50,000 ppm CO_2 and when the level dropped to 5,000 ppm CO_2 the desiccators would refill to 50,000 ppm CO_2 to begin the absorption cycle again. A summation of the number of cycles that occur would reveal the total amount of CO_2 absorbed by the concrete. A typical example of one absorption cycle is contained in Figure 2.4.

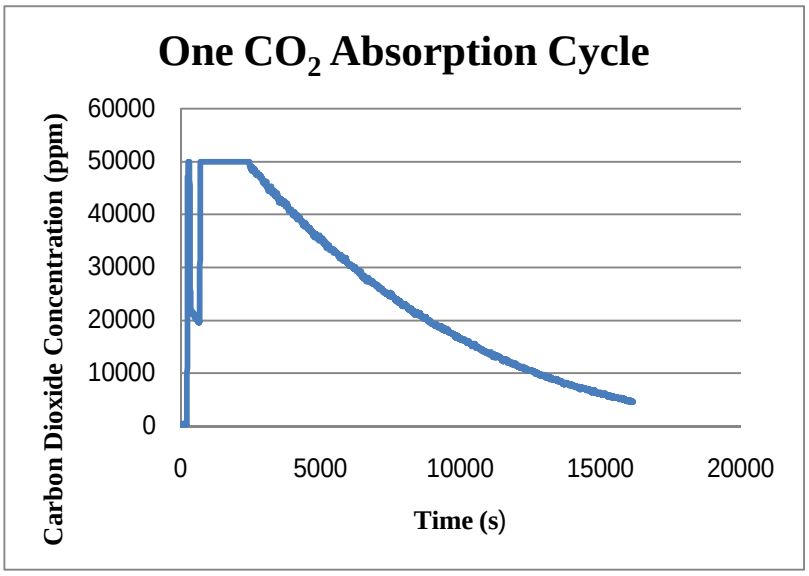

Figure 2.4 Example of one CO_2 absorption cycle. The summation of these cycles would yield the total CO_2 uptake.

An average CO_2 concentration reading would be taken every 30 seconds for 28 days and written to disk. A recarbonation time period of 28 days was needed so that full or close to full recarbonation could occur in the samples. This time frame would later change during the course of the study to 21 days. This was due to time constraints brought on by the delayed start of the testing. The construction of the experimental setup took place at the end of 2008 and beginning of 2009 with testing beginning at the start of September 2009.

Six desiccators would be wired together but able to operate independently, with each desiccator housing a single carbon dioxide specific infrared probe and the ability to fill and empty without interfering with neighbouring desiccators. Six desiccators would allow for two samples to be tested at a time with triplicate measurements taken for each sample. The desiccators used were six 2.5 L Perth Moncrieff desiccators and were obtained from the Chemistry Department at the University of Canterbury. The infrared probes were the same as those used in the Nordic Innovation Centre study. These were Vaisala GMT221 carbon dioxide infrared probes with a detection range of 0-5±0.2% CO_2 by volume. These probes were the best for the monitoring of the CO_2 concentration as they gave a large detection range and were relatively easy to use and incorporate into the design. The Vaisala GMT221 probes were purchased directly from Vaisala in Finland. A detailed diagram of the desiccator setup is shown below in Figure 2.5.

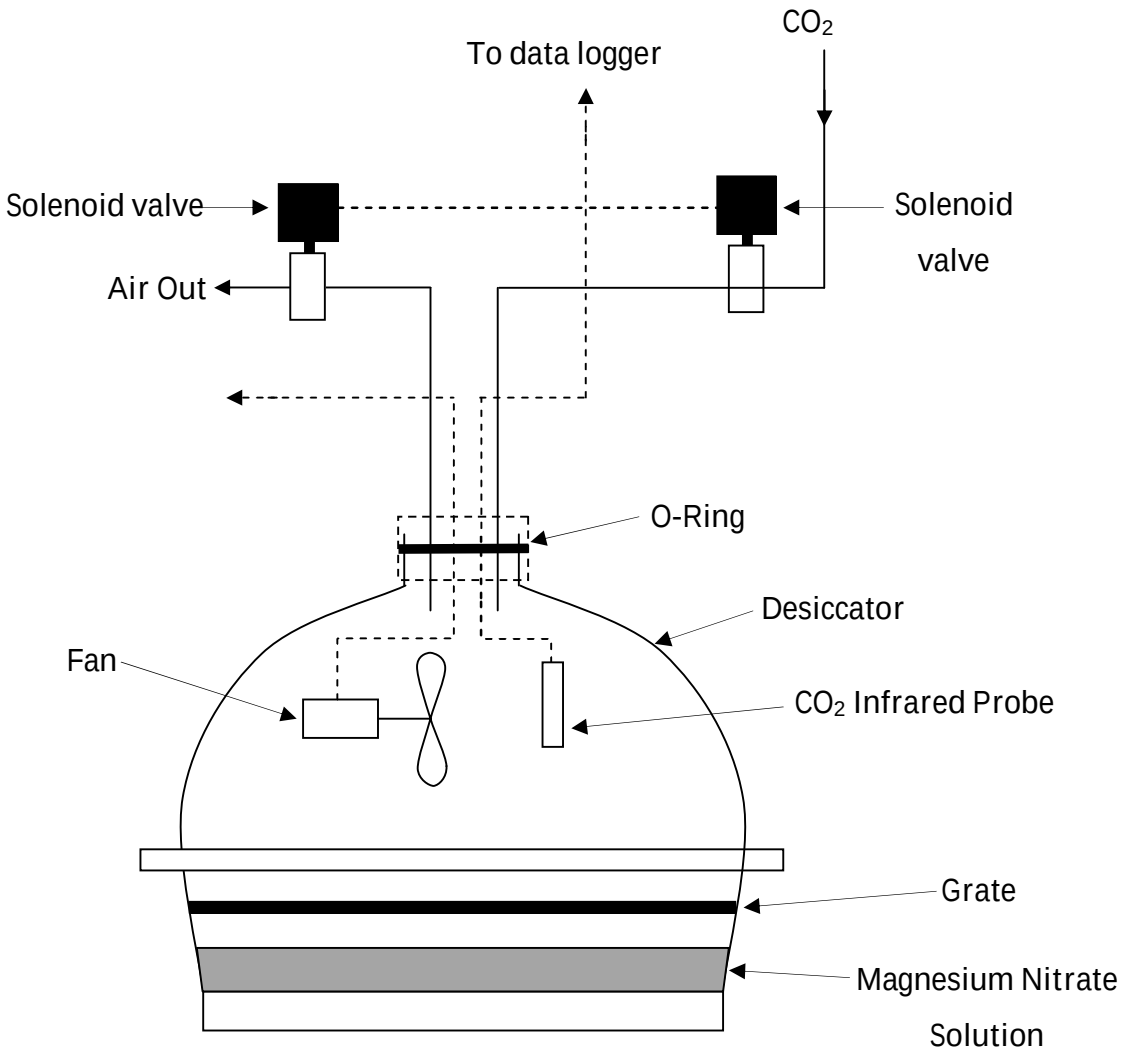

Figure 2.5 Cross section of desiccator showing probe, fan, solenoid valves, desiccator and other details.

There were two solenoid valves per desiccator. One allowed CO_2 in from a cylinder introduced at 0.2 bar and the other allowed air out so that the pressure in the desiccator would remain at one atmosphere. The pressure had to be very low so that the introduction of CO_2 into the desiccator could be controlled. The solenoid valves used were SMC VX21 DC and were purchased from the electrical supplier for the Chemistry Department.

The probe would be housed in the lid of the desiccator along with small electric fans to maintain a homogenous atmosphere inside the desiccator. The lids of the desiccators needed to be modified to accommodate the probes and fans. Modification of the desiccator lids was carried out by Mr Robert McGregor. He is the *in-house* glass blower for the Chemistry Department at the University of Canterbury. He created a small glass capsule that fitted onto the lid where the probe sat and was sealed using a screw cap. It was important that the modifications made did not affect the ability of the desiccator to create an airtight seal. Any CO_2 that leaks out of the desiccator would give a false CO_2 uptake reading. The integrity of the airtight seal was tested after the modifications had been completed. Each desiccator was sealed using silicon grease and G-clamps and filled to ~50,000 ppm CO_2. The CO_2 concentration was then monitored to see if any decrease occurred. The concentrations remained steady over a period of 10 hours and the airtight seals were deemed fit for testing. Figure 2.6 below shows a close up of the interior of the lid with the probe and fan attached.

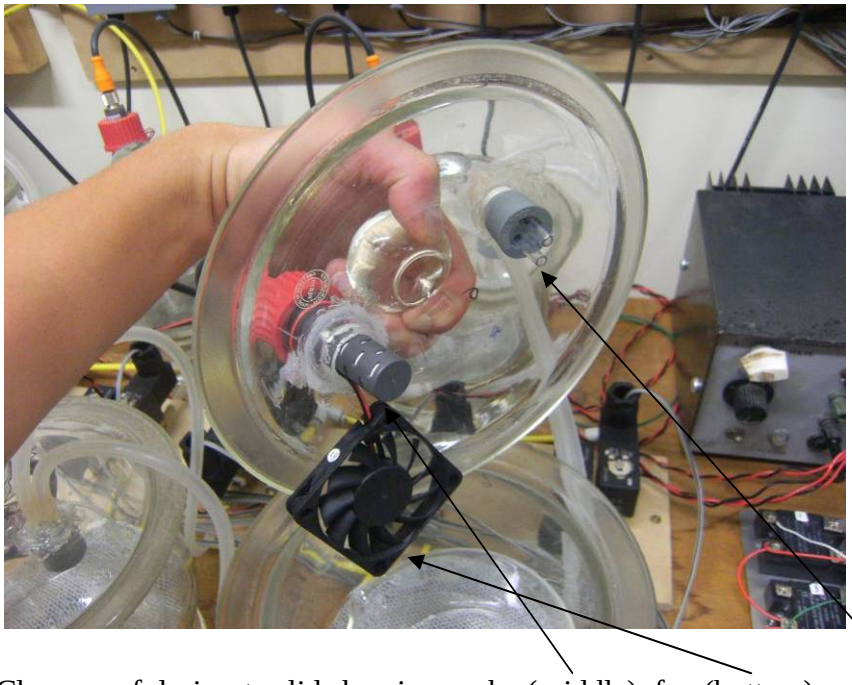

Figure 2.6 Close up of desiccator lid showing probe (middle), fan (bottom) and CO_2 inlet valves (top right).

The probes then fed into the probe housing mounted above the desiccators. From here each probe fed into a National Instruments USB6009 data-logger (Figure 2.7). This would take the carbon dioxide concentration, measured as an induced voltage and convert the signal from analog to digital. This digital signal could then be interpreted by the computer and logged.

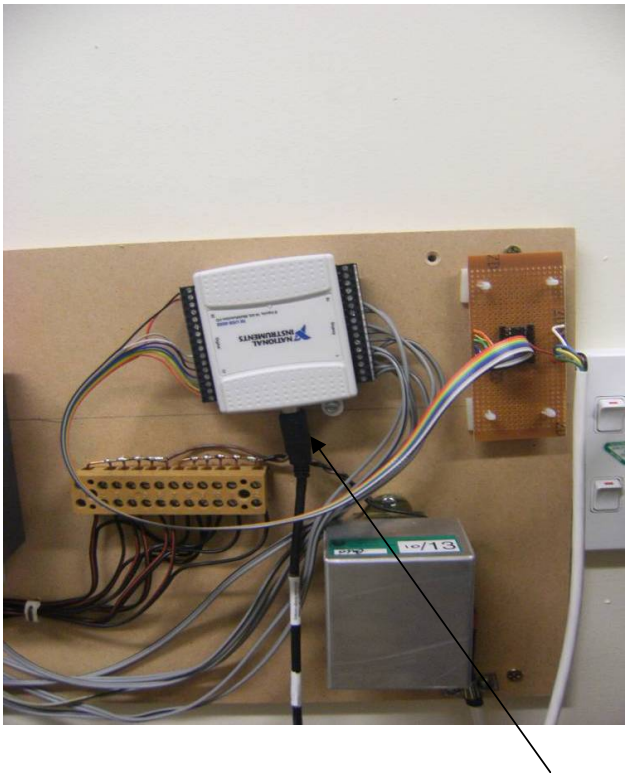

Figure 2.7 National Instruments USB6009 data logger (centre).

The experimental setup was to be automated as previously discussed and this required computer software that was capable of programming and data collection. Two software options were narrowed down. The first was National Instruments LabView and the second National Instruments Measurement Studio. National Instruments provided the best software for the task specified as it was easy to use and was capable of collecting and logging data and writing programmes for experimental control. It would also be easier to integrate the data-logger with the software as they came from the same manufacturer. For the system to be automated the computer would have to know when the CO_2 concentration was low and refill the desiccators while also recording the concentrations

and writing them to a file. National Instruments LabView Version 8.6.1 was chosen for the task as it allowed an array of programming options including automation and a practical interface.

Automation of the system in the beginning proved to be difficult. It was found that communication between the computer and the solenoids was not as easy as it was thought. Originally the plan had been to wire the data logger directly to the solenoid valves but this was not achieved as the data logger did not supply a sufficient voltage to operate the solenoids. After a month of trying to get the automated system working without success it was decided to test the suitability of having manual filling of the desiccators (see Fig 2.8).

Switches for each set of solenoid valves were installed and connected to a power supply. When the CO_2 concentration was low the switch would be flicked and it would refill. When the predetermined concentration was reached the switch would be turned off and CO_2 absorption could continue. The problem with a manual control was that the 20 MPa < 10 mm samples were absorbing 45,000 ppm CO_2 in a little over an hour. It was not practical to manually fill the desiccators every hour for 28 days so automation was necessary to achieve a good set of results.

Figure 2.8 Manual setup with switches bottom centre. Each desiccator had its own switch to remain independent.

With the elimination of the manual setup more options were considered for attempting automation. The best place to find expertise in the field of automation and programming was the Engineering Department at the University of Canterbury. Mr Julian Murphy is a technician in the Mechatronics Department at the University of Canterbury and had extensive experience in programming and using LabView. He came to look at the setup and revealed how the setup could be automated and proper data collection solved (a circuit diagram of the LabView control system is contained in Appendix 1). He identified the cause of the problem and showed how automation could be achieved. This was done by running the output signals from the data logger through six solid state relays that could increase the output voltage of the data logger sufficiently that the solenoid valves could be opened and closed. These would in turn be automatically controlled by the LabView programme. The solid-state relays used were Hongfa HFS33 (JG-33F) solid state relays (Figure 2.9).

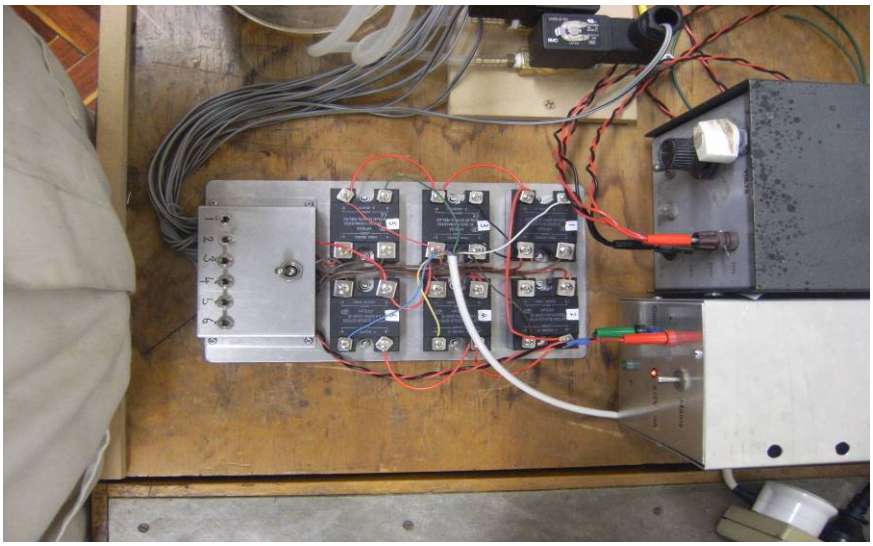

Figure 2.9 Close up of the six solid state relays installed to boost the voltage to the solenoid valves.

The construction of the automated setup was completed in August 2009 (see Fig. 2.10). The first samples were placed in at this time as a practice run to see how the setup functioned and ensure all the components were working correctly. The setup worked well and data collection and refilling of the desiccators went according to plan. Two weeks into the first automated run the computer's display drivers crashed. This was unexpected and proved to be a serious problem as the computer did the same thing upon trying a second run. This problem most likely occurred because the computer was an old machine and appeared to struggle to run the LabView programme even though it met all the recommended requirements specified by National Instruments.

The computer administrator Mr John Davis in the Chemistry Department was able to source a newer computer to solve this problem. This was far superior to the first computer used and was installed in August 2009. A third practice run was carried out at the end of August 2009 and no problems were encountered as before in the two week practice run. With the setup completed testing of the crushed concrete specimens began in September 2009.

Figure 2.10 Overview of automated setup with crushed concrete samples in desiccators and solid state relays in the bottom right.

There were many problems encountered in the construction of the apparatus, of which some have been mentioned above. The problem of automation for the setup took a long time to sort out due to the lack of expertise available at the beginning of the construction. There were also multiple problems with the first computer used. It would crash during test runs due to display driver errors and would execute random commands that had not been programmed to occur at that particular moment. The introduction of a new computer to run the experiment appeared to solve these problems that were being encountered with the first computer and random crashes were now a thing of the past.

Another problem that increased the lead time of the experiment much further than anticipated was the actually programme used to control the experiment. LabView was a new programme that few people in the University were familiar with. Interfacing with the solenoid valves and the saving of the raw data into appropriate file formats was not accomplished to the desired specifications. It was after many months of unsuccessful attempts to get the setup working it was decided that more expertise was needed in the programming and automation area. With the help of Mr Julian Murphy the automation process was revealed to need solid-state relays to make the solenoid valves open and close correctly. Mr Murphy also identified a corrupted file in the initial LabView

programme which may have been a cause of the data not writing to the hard disk correctly. With the help of Mr Julian Murphy, the LabView programme and experimental apparatus were completed in time for a quick trial of the new setup to be carried out. There were no problems after the corrections to the LabView programme and addition of the solid-state relays. The automated setup worked well although there were still some refinements that could have been made to it if time had permitted and these are discussed in Section 4.2.

2.5 Other Methods of Recarbonation Analysis

Other methods were also used to confirm that recarbonation had taken place by detection of the recarbonation product calcium carbonate using FTIR and TGA. Weight gains of the samples were also used to compare to the probe results and phenolphthalein indicator was used as a quick visual check to show recarbonated areas of the concrete samples.

The recarbonation reaction yields calcium carbonate as the main product. FTIR is a very effective method to show the evolution of the carbonate ion (CO_3^{2-}). It has a characteristic absorption peak in the wave number range of 1410-1510 cm^{-1} [30,32,34]. Cement mortar samples were taken before and after testing and FTIR spectra taken for each. If recarbonation has occurred then there will be an increase in the absorption in the corresponding wave number range of 1410-1510 cm^{-1}. The spectrometer used was a PerkinElmer Spectrum One FT-IR Spectrometer and located in the Chemistry Department at the University of Canterbury.

It has been well demonstrated that calcium carbonate decomposes in the temperature range of 500-950 ºC [31-33]. TGA can be used on mortar samples from the crushed concrete both before and after CO_2 exposure. If recarbonation has taken place then the weight loss in the above temperature range should increase after testing. The same temperature range should exhibit little weight loss prior to testing, as the concrete had not undergone recarbonation. The TGA apparatus used was a TA Instruments SDT Q600 located in the Chemistry Department at the University of Canterbury.

Since recarbonation involves the absorption of CO_2 the crushed concrete samples were weighed before and after testing. The absorption of CO_2 by the crushed concrete can

potentially be significant. Therefore, if a significant quantity of CO_2 is absorbed a weight increase should be observed. Assuming all weight gained by the crushed concrete sample is due to CO_2 then the weight can be used as a direct comparison to the uptake calculated by the infrared probes.

Phenolphthalein indicator is a tried and tested method for detecting carbonation of concrete [3,5,6,30]. The phenolphthalein remains colourless on carbonated concrete and turns pink on recarbonated concrete (above pH 10). It has been demonstrated that this method is not good for determining the carbonation boundary as it is not a sharp front but a gradual one, but is useful as a visual aid to see where significant recarbonation has occurred on the sample.

3.0 Results and Discussion

3.1 Theoretical Uptakes

The XRF analysis of the cement can be used to calculate different theoretical CO_2 uptakes (Tables 2.3 and 3.2). XRF analysis allows the effective oxide weight percentage of CaO to be ascertained. Theoretically all the CaO present in the cement mortar can undergo recarbonation but this is not always the case. Due to the hydration rates of ($3CaO.SiO_2$) and ($2CaO.SiO_2$) being very different, full hydration takes a long time to achieve. Papadakis *et al.* (1989*)* described the rates at which concrete hydrates and this information is summarized in Table 3.1. Even after a long period of time some ($3CaO.SiO_2$) and ($2CaO.SiO_2$) will remain. This means that not all the CaO that was originally in the cement will be available for recarbonation. Calculating the theoretical CO_2 uptakes allows a comparison to be made with the actual CO_2 uptakes. This can help identify how much of the total CaO content may be undergoing recarbonation and also how the recarbonation reaction has progressed.

The assumptions made in this calculation are that the reaction proceeds according to equation **(13)** and that only the CaO containing compounds are available for recarbonation. The theoretical uptake for a given percentage of recarbonated CaO from the cement is listed in Table 3.2.

$$CaO + CO_2 \bullet \quad CaCO_3 \qquad \textbf{(13)}$$

Time (days)	Percent Hydrated	
	($3CaO.SiO_2$)	($2CaO.SiO_2$)
100	95	80
1,000	96	93
10,000*	100	97
100,000*	100	100

Table 3.1 C_3S and C_2S hydration rates represented as a percentage hydrated with respect to time. [23]. *extrapolated data

Strength	CaO Content %	% CaO Recarbonated	Total CO_2 Uptake (g CO_2/kg cement)
20 MPa	63.8	100	500
		75	375
		50	250
40 MPa	64.1	100	503
		75	377
		50	251

Table 3.2 Theoretical total CO_2 uptakes for cement used in 20 MPa and 40 MPa preparation according to percentage of CaO recarbonated.

From Table 3.2 it is clear that if both design mixes were to undergo full recarbonation they would absorb a little over 500 g CO_2/kg cement each. This is unlikely to be achieved as full hydration will not be achieved in the time frame of this study. A more realistic uptake is in the 50-75 % range. This would still equate to 50-75 % reabsorption of the calcination CO_2 emissions.

The CO_2 emissions for one tonne of cement in New Zealand are 850 kg (Section 1.1 and 1.2). Calcination emissions were believed to be responsible for half of this release. From Table 3.2 it can be seen that 1 kg of cement has a theoretical uptake of approximately 500

g CO_2. This means that the calcination emissions are more likely to be responsible for 60 % of the total CO_2 released in manufacture.

The total uptake could also be calculated with respect to the cement content of the concrete. Since the quantities of cement used in each design mix is known it can be assumed that all the cement is evenly distributed through all the concrete at the same concentration as when mixed. With the knowledge of the cement mass used, the mass of CaO in a concrete sample of any weight can be established.

3.2 Infrared Probe Recarbonation Calculations

The CO_2 detection by the infrared probe was calculated as a summation of each absorption cycle of 45,000 ppm CO_2. This would yield the total CO_2 uptake by the crushed concrete as measured by the probes. For this calculation to be completed the concentration of CO_2 needed to be converted to a mass of CO_2 that was absorbed for each cycle. The Ideal Gas Law (Equation **(14)**) was used for this conversion. This was a straightforward calculation for all elements of the equation were known except for the mass of CO_2.

$$PV = nRT \qquad \textbf{(14)}$$

As the gas constant, pressure and temperature of the room were already known (Section 2.4) the only calculation needed was that of the volume that the CO_2 occupied. The CO_2 concentration was measured with respect to volume so the volume that 5 % CO_2 occupied was calculated. The desiccators were stated to have a volume of 2.5 L. To make sure this was the case the desiccators were filled with water until full. The amount of water used to fill the desiccator would be equal to the total volume of the desiccator. This was done with each desiccator and the results of this are listed in Table 3.3. The volume occupied by the concrete samples and equipment such as the fans and probes was estimated to be ~250mL. This added an uncertainty to the measuremnt calculations of 10% as this was not deducted from the total volume of the desiccator. 5 % of 2.5 L is 0.125 L, which is the

volume that 50,000 ppm CO_2 occupies at one atmosphere inside the desiccator. The desiccator is refilled when the CO_2 concentration reaches 5,000 ppm so each absorption cycle the crushed concrete is actually absorbing 45,000 ppm. Using Equation (14) the mass of 45,000 ppm CO_2 in the desiccator is equivalent to 0.0047 mol or 0.206 g. Therefore during each absorption cycle the crushed concrete sample is theoretically absorbing 0.206 g CO_2.

Desiccator	Total Volume ±5 mL
1	2495
2	2498
3	2510
4	2503
5	2491
6	2508
Mean	**2500.83**

Table 3.3 Volumes of the six desiccators with the average volume stated at the bottom of the table.

3.3 CO_2 Specific Infrared Probe Results

The design mix for 20 MPa concrete was the first to be tested, followed by the 40 MPa immediately after, during the months of November and December 2009. This start was originally planned for much earlier in the year but was delayed due to problems encountered in the construction and programming of the experimental setup.

Each design strength comprised of four different particle sizes of <10 mm, <20 mm, <40 mm and uncrushed. The testing was done in two runs with the <10 mm and <20 mm samples being tested in the first run and <40 mm and uncrushed samples in the second run. After completion of the sample preparation as described in Sections 2.1-2.2, a 500 g sample was weighed out for each desiccator. The samples were then exposed to the enriched CO_2 atmosphere inside the desiccator for a period of 21 days. After testing the samples were re-weighed and tested for CO_2 penetration using phenolphthalein indicator. Cement mortar samples were taken from the cement particles for FTIR and TGA analysis. Each particle fraction would contain triplicate probe measurements and the average of the three would be taken for analysis.

The probe values measured were recorded automatically by the LabView software and when testing was completed were analysed in Microsoft Excel to establish any relationships. An average of the triplicate measurements was used to determine the average uptake for each particle size and these results are presented below. In the previous section it was discussed how the probe results would be the summation of all the absorption cycles. This would reveal the total CO_2 for each sample and the amount of CaO that had undergone recarbonation. A summary of the infrared probe results are contained in Table 3.3.

Strength	**CaO Content (%)**	**Sample**	**Total CO_2 Absorbed (g) ±0.5 g**	**Absorption (g CO_2/kg cement) ±1.1 g**	**% Calcination Emissions Absorbed**
20 MPa	63.8	<10 mm	21.8	420	83
		<20 mm	18.8	360	72
		<40 mm	3.1	60	12
		Uncrushed	2.3	43	9
40 MPa	64.1	<10 mm	18.3	350	70
		<20 mm	15.0	290	57
		<40 mm	2.5	47	9
		Uncrushed	1.9	36	7

Table 3.3 CO_2 uptake data for 20 MPa and 40 MPa samples shown as total CO_2 uptake by 500 g sample and CO_2 uptake with respect to cement content.

The most obvious result was that the 20 MPa design mix with water/cement (w/c) ratio of 0.67 absorbed considerably more CO_2 that the 40 MPa design mix of water/cement ratio 0.49. This was in agreement with the literature results that claimed that the higher the w/c the greater the extent of recarbonation [3,10-20]. The 20 MPa <10 mm crushed sample

absorbed the most CO_2 of all the samples tested, with an average total absorption of 21.8 g for a 500 g sample over 21 days. The <20 mm also exhibited a significant uptake of 18.8 g CO_2. The <40 mm crushed samples and the uncrushed samples demonstrated very low total average absorptions of 3.1 g and 2.3 g CO_2, respectively. These can be seen clearly in the 20 MPa and 40 MPa probe graphs in Figure 3.1-3.2. This low uptake may be explained by the particle size distributions. The <10 mm and <20 mm samples had large fractions of particles that were less than 8 mm in one dimension as opposed to the <40 mm samples that had only a small percentage of particles below 8 mm. To test this theory phenolphthalein indicator was used to see whether the inside of the <40 mm particles had undergone recarbonation (Section 3.4). The uncrushed result was not a surprise as its total CO_2 absorption was predicted to be low due to its small surface area.

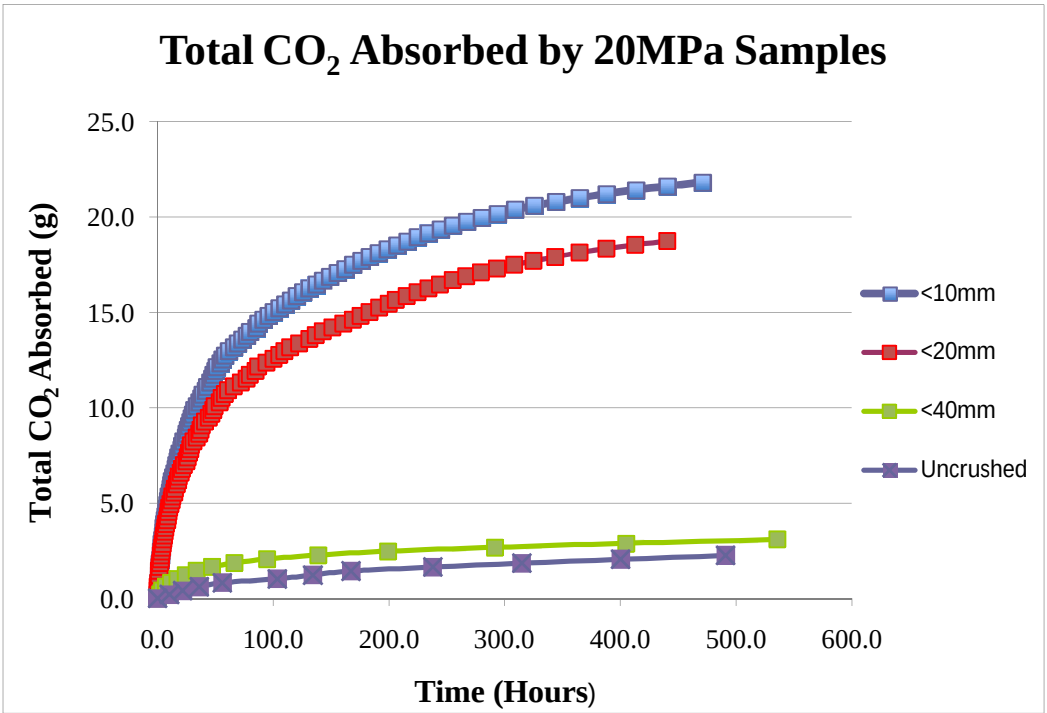

Figure 3.1 Total CO_2 absorbed by 20 MPa for samples <10, <20, <40 mm and uncrushed as measured by IR probes.

A similar pattern was also observed for the 40 MPa samples after 21 days. The largest total CO_2 uptake was observed for the <10 mm. This sample had a total average uptake of 18.3 g of CO_2. This was not as high as the uptake seen for the 20 MPa <10 mm samples.

The 40 MPa samples were expected to have a lower uptake than the 20 MPa samples as shown in previous studies [10-15]. The <20 mm samples absorbed 15.0 g CO_2 in the same time period. As seen in the 20 MPa results the uptake for the <40 mm and uncrushed samples was very slow. The total average uptakes observed by the <10 mm and <20 mm samples were 2.5 g and 1.9 g CO_2. The results for the total uptake were verified by weighing the samples before and after testing. The results for this are contained in Section 3.4.

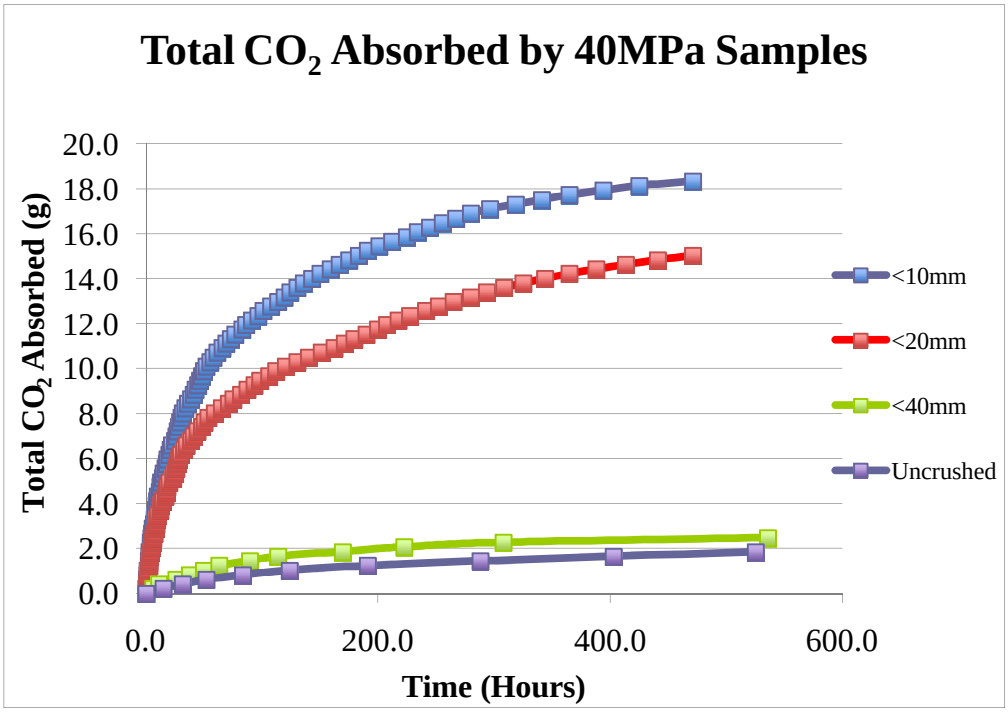

Figure 3.2 Total CO_2 absorbed by 40 MPa for samples <10, <20, <40 mm and uncrushed as measured by IR probes.

In terms of the original calcination emissions released during manufacture it was assumed that the original cement content of the concrete would be evenly distributed throughout the concrete samples. This gave each 20 MPa sample a cement content of ~10% and the 40 MPa samples a cement content of ~14%. An assumption was also made regarding the amount of CO_2 released from the calcination process. It was assumed that all CaO present in the cement had released CO_2 during manufacture and this was solely responsible for the calcination CO_2 emissions. The results for this are shown in Table 3.3 above.

The <10 mm 20 MPa sample reabsorbed 83 % of the original calcinations emissions. The <20 mm and <40 mm samples for 20 MPa showed 72 % and 12 % absorption of the calcinations emissions respectively. The reabsorption of the calcinations emissions was similar in the 40 MPa samples but the extent of absorption was not as high as the 20 MPa samples. The particle sizes of <10 mm, <20 mm and <40 mm absorbing 70 %, 57 % and 9 % of the original calcinations emissions respectively.

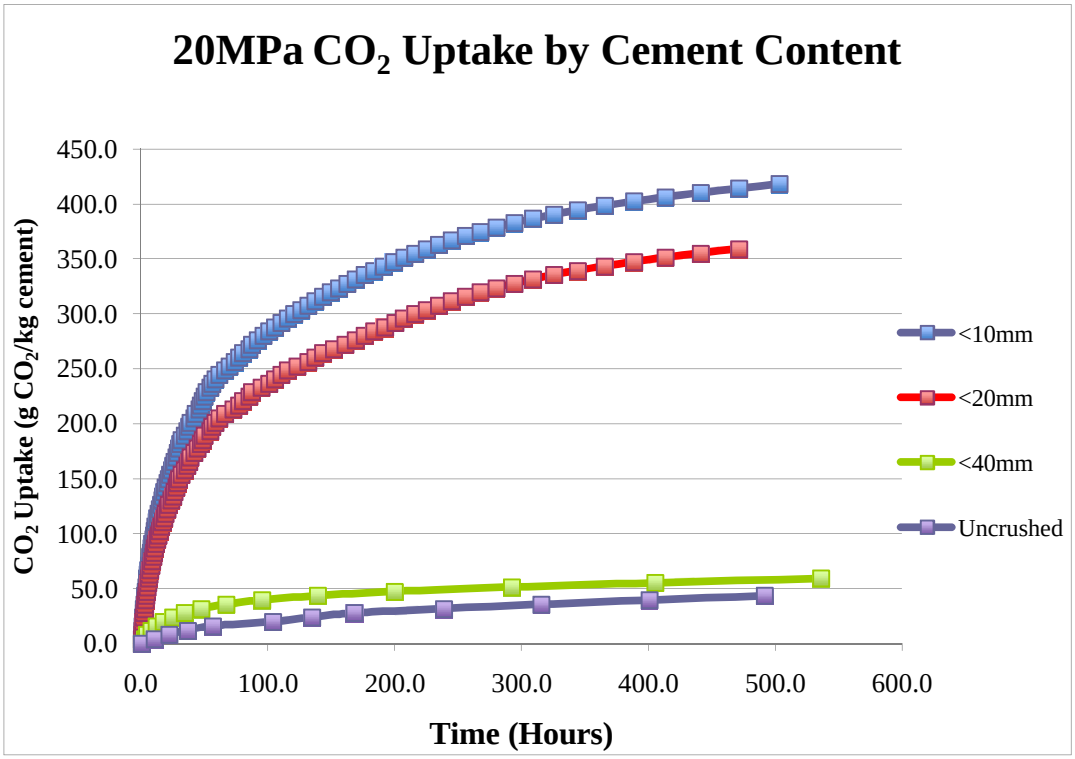

Figure 3.3 CO_2 Uptake by cement content of 20 MPa samples for sizes <10, <20, <40 mm and uncrushed.

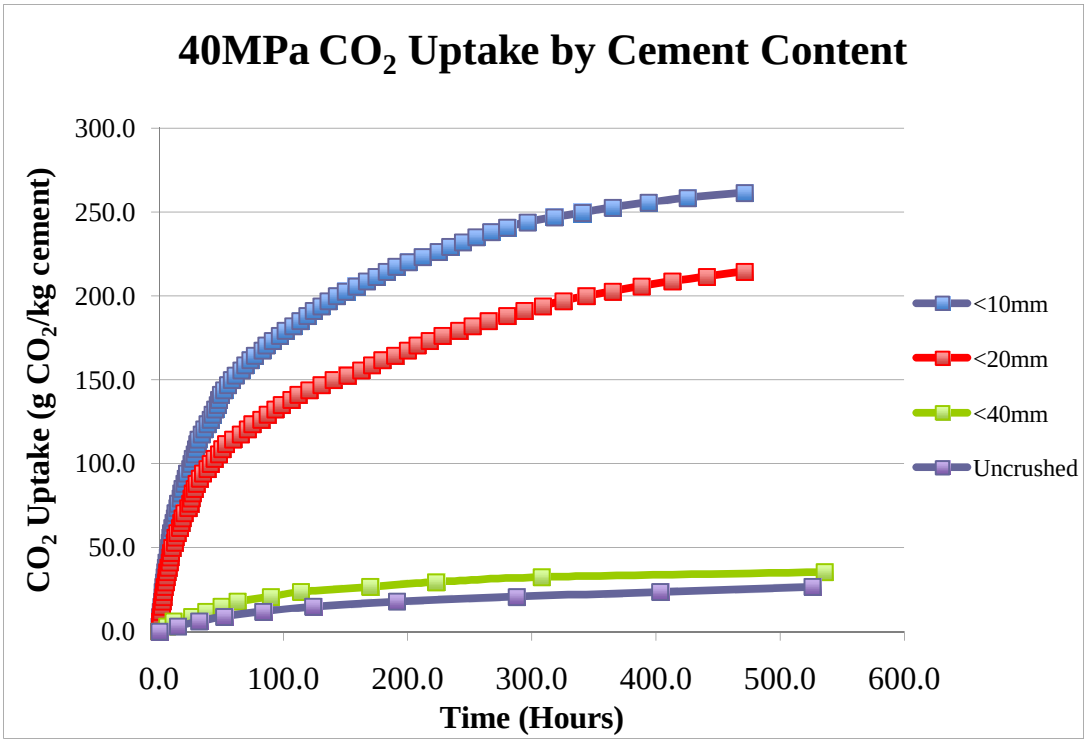

Figure 3.4 CO_2 Uptake by cement content of 40 MPa samples for <10, <20, <40 mm and uncrushed.

The information in Table 3.3 also allows the theoretical percentage of CaO that has been recarbonated to be determined. Using the CaO content of the cement and the uptakes with regard to cement content (Figures 3.3-3.4), the CaO that had undergone recarbonation could be calculated. The results of this analysis are contained in Table 3.4. From this table it can be seen that the 20 MPa samples show a maximum recarbonation of CaO of 83 %. This is for the <10 mm sample. The same particle size for 40 MPa revealed that 70 % of the CaO in the cement had undergone recarbonation. The <20 mm samples for both strengths also exhibited significant recarbonation of the CaO in the cement. The <40 mm and uncrushed samples also had CaO that had undergone recarbonation but this was minute in comparison to the <10 mm and <20 mm samples.

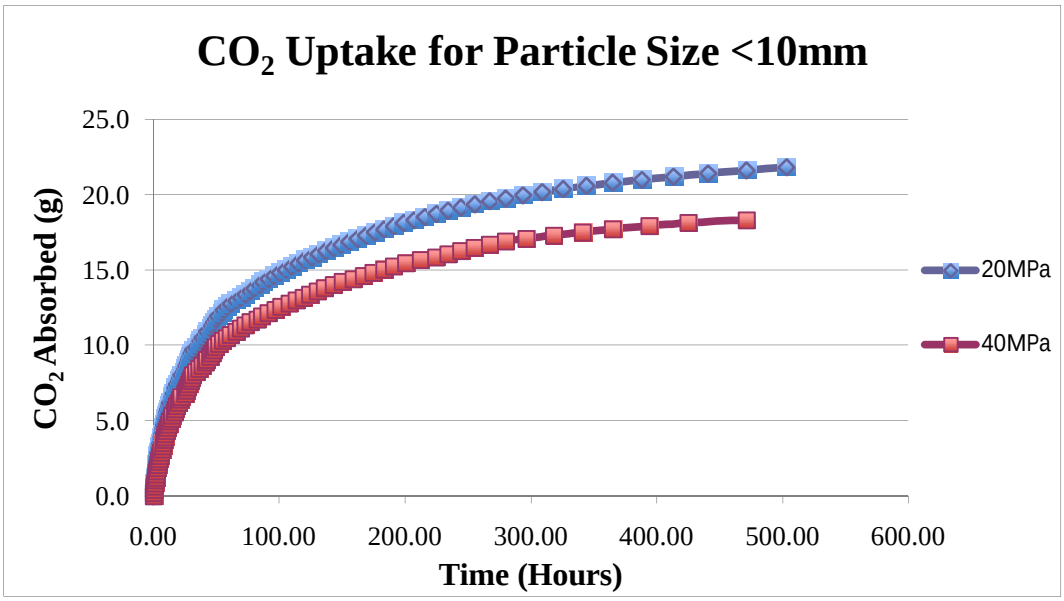

Figure 3.5 Comparison of CO_2 uptake of <10 mm particle size for 20 MPa and 40 MPa design mixes.

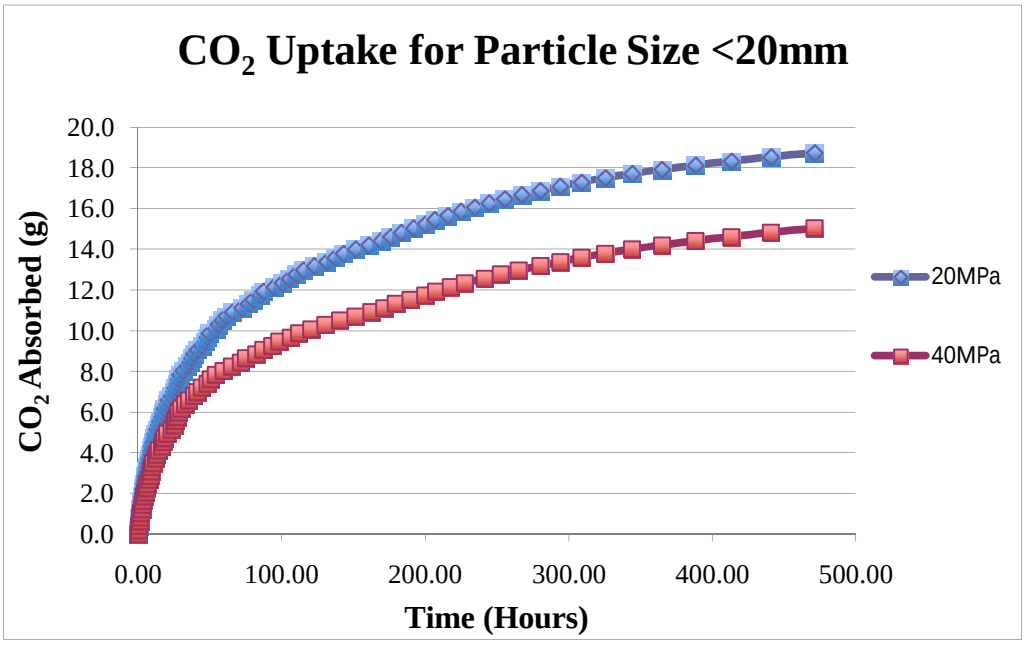

Figure 3.6 Comparison of CO_2 uptake of <20 mm particle size for 20 MPa and 40 MPa design mixes.

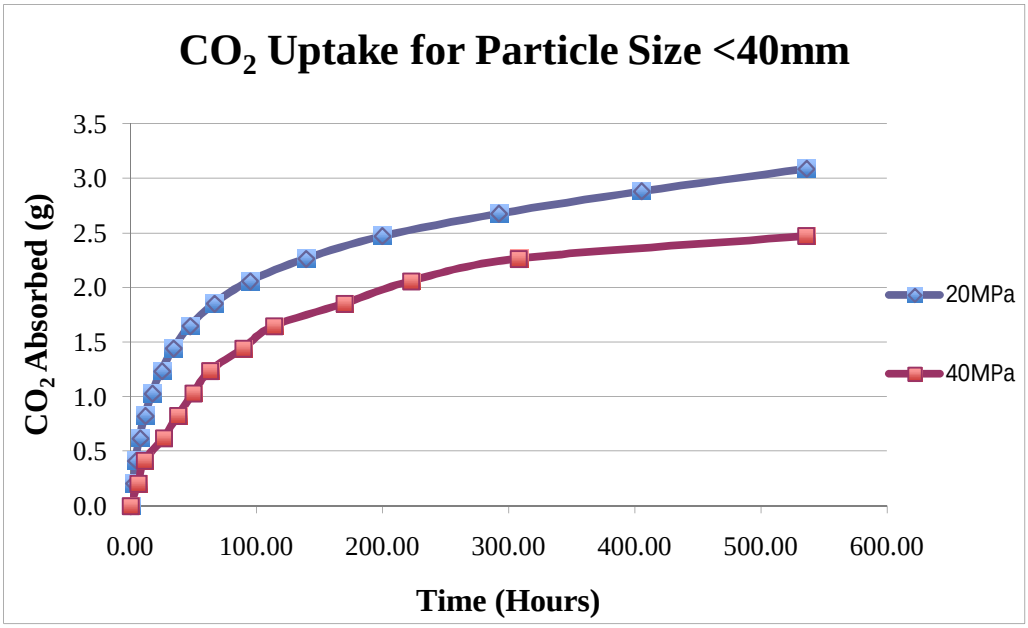

Figure 3.7 Comparison of CO_2 uptake of <40 mm particle size for 20 MPa and 40 MPa design mixes.

3.3.1 CO_2 Specific Infrared Probes Summary

Carbon dioxide specific infrared probes proved to be a very effective tool in measuring the CO_2 uptake of crushed concrete. Two design mixes of 20 MPa (w/c 0.67) and 40 MPa (w/c 0.49) were tested for particle sizes of <10 mm, <20 mm, <40 mm and uncrushed. All particle sizes exhibited recarbonation but it was the smaller particle sizes for both strength designs that demonstrated significant CO_2 absorption. It must also be noted that 80-90 % of the CO_2 aborbed occurred within the first 10 days of exposure. After 10 days the recarbonation rate appeared to diminish considerably. The results were similar to those found in the Nordic Innovation Centre study [10]. They found that 60-80 % of the calcination emissions could be reabsorbed for concrete mixtures with w/c of 0.6 or higher for grain size 1-8 mm within 20-35 days of exposure. The 20 MPa design mix used in this study had a w/c of 0.67 and reabsorbed 83 % of the original calcination emissions for a particle size <10 mm. Although the w/c of the Nordic design mix was slightly lower than the w/c used in this study, the particle size and exposure time was similar. The Nordic sample abosrbed a maximum of 80% of the calcination emissions compared with 83%

found in this study. The difference may be explained by the w/c ratio being lower in the Nordic mix which would in turn lead to a slower recarbonation rate than a w/c of 0.67.

The 20 MPa design mix had greater uptakes of CO_2 than the 40 MPa design mix for all particle sizes (Figure 3.5-3.7) and this also agreed with the findings in the Nordic Innovation Centre study that found that the higher the strength (lower w/c), the lower the recarbonation rate [10]. This was in agreement with previous research that had showed that the recarbonation rate increased with decreasing strength which primarily attributable to porosity. The maximum average amount of CO_2 absorbed was by the 20 MPa <10 mm sample which absorbed 21.83g CO_2. This equated to 83 % of the original calcination emissions being reabsorbed and 83 % of the cement CaO undergoing recarbonation. On the other hand the 40 MPa <10 mm sample absorbed a maximum of 18.33 g CO_2 that revealed 70 % of the original calcination emissions had been reabsorbed.

The results for the <20 mm samples were similar but due to the smaller surface area available for recarbonation the uptake was smaller than the <10 mm samples. The 20 MPa <20 mm samples absorbed an average maximum of 18.75 g CO_2 and corresponded to 72 % of the calcination emissions being reabsorbed. 72 % of the CaO had also undergone recarbonation. The equivalent 40 MPa samples absorbed a maximum of 15.04 g CO_2 and showed 57 % of the CaO had undergone recarbonation.

The <40 mm and uncrushed samples exhibited very low CO_2 uptakes due most likely to the very small surface areas and a lack of particles that were less than 8 mm. This was also found in the Nordic Innovation Centre project that claimed that very low recarbonation rates were achieved for particle size of >16 mm. Crushed concrete particles of sizes below 8 mm have been shown to have a very rapid recarbonation rate [5]. The <40 mm samples for 20 MPa and 40 MPa absorbed 3.09 g and 2.47 g of CO_2 respectively. This equated to 12 % and 9 % recarbonation of the CaO in the cement. The uncrushed samples had the lowest CO_2 absorption rates with both design strengths unable to absorb more than 2.27 g of CO_2 in 21 days. This confirmed what engineers have said in that intact concrete that is not crushed has a very slow recarbonation rate. This also showed that crushing of concrete increases the recarbonation rate substantially.

When looking at the reactions and theory of recarbonation on paper it appears that the 40 MPa design mix should absorb more CO_2 than the 20 MPa design mix because it has a greater cement content. This was not the case and can be explained by the porosity and

density of the concrete. In Section 1.5 it is mentioned that the porosity of the concrete has a big influence on recarbonation rate [5]. Because the concrete strength is inversely proportional to porosity, a low w/c (40 MPa) will be less porous than a high w/c (20 MPa). Because the CO_2 has to diffuse into the concrete the more porous the concrete is the faster it will recarbonate. Therefore, the 20 MPa design mix will recarbonate faster than the 40 MPa design mix as was observed.

The particle size has the greatest influence on the recarbonation rate. The smaller the particle size the greater the CO_2 aborption. The concretes w/c was also found to be a factor influencing CO_2 uptake, as the w/c of 0.67 (20 MPa) demonstrated a much larger recarbonation rate than that of the concrete samples with w/c of 0.49 (40 MPa).

.3.4 Weight Gain and Phenolphthalein Indicator Results

The CO_2 that had been absorbed by the concrete needed to be calculated using a different method so that the accuracy of the probes could be ascertained. The most simple method was to simply weigh the samples before and after recarbonation testing to quantify the weight gain brought about by CO_2 absorption [3,5,6,30]. This assumed that all the weight gain of the crushed concrete samples was from the absorption of CO_2. The <40 mm samples for both design strengths demonstrated very low uptakes. This was thought to be due to the small surface area of the sample and the lack of particles in the size range below 8 mm. To test how much recarbonation had taken place the particles of each test were cut in half (if possible) and sprayed with phenolphthalein indicator solution (0.5% phenolphthalein in 50% ethanol 50% water**).** The indicator would turn bright pink on uncarbonated concrete (pH > 10) and remain colourless where the concrete had recarbonated (pH < 10).

The results of the weighing of the samples before and after testing are given in Table 3.4. Also included in this table is the weight gain measured by the infrared probes as a comparison. It can be clearly seen that the weight as measured by the probes is always slightly more than that measured by weighing the samples on a scale. However, despite this descrepency the values are still in relatively good agreement.

The difference may be due the uncertainty in the probes measurements. The probes were rated at 0-5 ± (0.02% + 2% of reading)% CO_2. The most likely cause of this discrepency is the fact that the volume of the concrete sample and the equipment inside the desiccator was not taken into account in the probe calculations. These components would take up ~250 mL of the desiccator volume so the values calculated for the probe uptakes are overestimated by ~10%. This could account for the discrepencies as all the differences between the two methods is within 10% except for the values of the 20 MPa uncrushed sample.

Sample		**Weight Gained (g) ± 0.005**	**Probe Weight Gain (g) ± 10%**	**Difference (g)**
20 MPa	<10 mm	20.65	21.83	1.18 (5.4%)
	<20 mm	17.39	18.75	1.36 (7.3%)
	<40 mm	2.86	3.09	0.23 (7.4%)
	Uncrushed	1.92	2.27	0.35 (15.4%)
40 MPa	<10 mm	17.45	18.33	0.88 (4.8%)
	<20 mm	14.12	15.04	0.92 (6.1%)
	<40 mm	2.30	2.47	0.17 (6.9%)
	Uncrushed	1.81	1.85	0.04 (2.2%)

Table 3.4 Comparison of weight gains for crushed concrete samples as measured by infrared probes and weight gain with the differences listed between the two methods listed in the right column.

The crushed samples of <10 mm and <20 mm for both design strengths exhibited behaviour that was expected of crushed concrete. The <40 mm samples though showed very low rates of recarbonation in comparison. To test why this may be a phenolphthalein indicator test was carried out. If the centre of the crushed concrete particles turned a bright pink this would mean that the pH was still above 10 and significant recarbonation had not occurred. If the indicator remained colourless than the pH had dropped below 10

and recarbonation had occurred [30]. The results of this test are contained in Figures 3.8-3.11.

Figure 3.8 Phenolphthalein test of <10 mm samples for both design strengths. Note all the particles are colourless indicating pH is below 10 and full recarbonation has occurred.

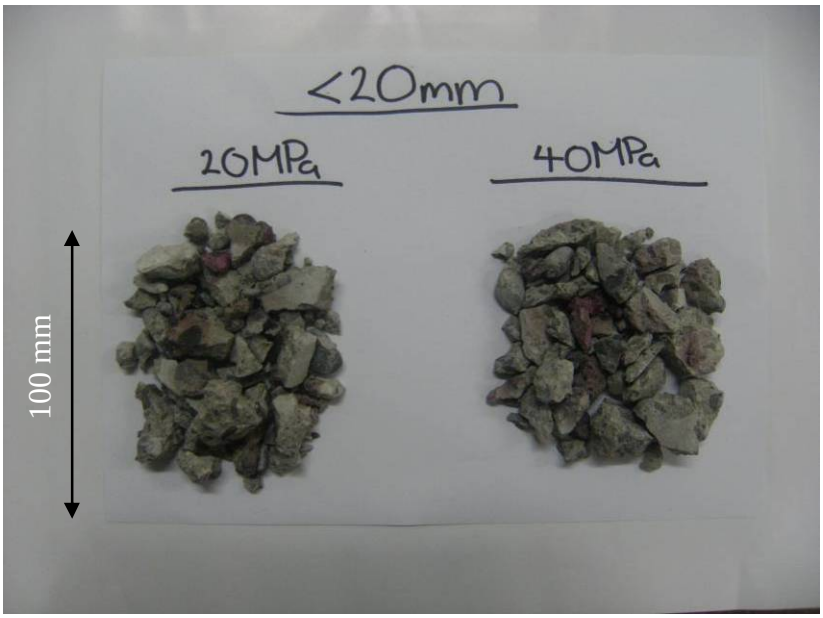

Figure 3.9 Phenolphthalein test of <20 mm samples for both design strengths. Note all the particles are colourless except for a small proportion of particles that have pink colouration. Indicates almost full recarbonation has been achieved.

Figure 3.10 Phenolphthalein test of <40 mm samples for both design strengths. Note all the particles exhibit pink colouration on their interior and remain colourless on the exterior. This shows that the outside of the particles has recarbonated but CO_2 has yet to penetrate right into the particles.

Figure 3.11 Phenolphthalein test of uncrushed samples for both design strengths. Note the centre of the samples is bright pink and uncarbonated. Only the outside of the sections is colourless and has undegone recarbonation.

The <10 mm samples for both design strengths remained colourless when sprayed with phenolphthalein indicator. This meant that the particles were all below pH 10. This indicated that significant recarbonation had occurred and supported the infrared probe results. The same colourless result was also observed for the <20 mm samples although small areas of pink were found on patches of some of the particles. This would indicate that most of the concrete matrix had undergone recarbonation except for some small areas where the CO_2 had yet to penetrate. This also supported the infrared probe results as the uptake for <20 mm samples was not as pronounced as the <10 mm samples but was still significant compared to the <40 mm and uncrushed samples.

A strong pink colour was observed on large areas of the <40 mm particles for both design strengths. This provided evidence that the infrared probe results were accurate in their assessment of low recarbonation rates for the <40 mm samples. Only small areas, most notably the exterior of the <40 mm particles, remained colourless and the interior was still pink. Some of the smaller particles in the <40 mm fractions had recarbonated substantially, but most of the large particles still had uncarbonated areas. This revealed that particle size was a determining factor in the recarbonation rate of crushed concrete.

The uncrushed samples exhibited a large bright pink area in the centre of the cylinder section. This showed recarbonation had only occurred around the edges of the section and that thecentre was still uncarbonated. This supported engineers' claims that concrete when *in-situ* carbonates very slowly.

3.4.1 Weight Gain and Phenolphthalein Indicator Summary

The weight gains as measured by the infrared probes were checked for their accuracy by weighing the samples before and after testing. Assuming all the weight gain associated with crushed concrete samples was from CO_2 absorption a comparison could be made.

The weight gains measured by the infrared probes were higher than those measured by weighing the samples before and after testing. The difference in the uptakes ranged from 5-8 % except for the <20 mm uncrushed sample, which had a difference of 15 %. There were possible reasons for the descrepency such as uncertainty in the infrared probe measurements and the volume of the concrete samples and equipment inside the desiccators was not included in the calculations. This would give an uncertainty of ~10 % which would account for the differences observed between the two methods.

The phenolphthalein indicator tests (Figures 3.8-3.11) allowed the identification of areas that had been recarbonated and those that had not. It was a simple visual test to see if the recarbonation rates observed by the infrared probes were representative of the true recarbonation that had occurred. The test showed that the <10 mm particles remained colourless and most of the <20 mm particles also remained colourless. This supported the infrared probe results, that considerable recarbonation had occurred in these particle sizes. The <40 mm and uncrushed samples demonstrated large areas of pink colouration that indicated it was a pH above 10. This indicated that only a small amount of recarbonation had taken place in these samples, which was backed up by the probe results.

3.5 TGA and FTIR Results

TGA and FTIR were used to establish if the $CaCO_3$ present in the concrete matrix had increased as shown in equations **(6-9)**. The liberation of the CO_2 molecules from $CaCO_3$

exhibits a distinctive TGA curve in the temperature range of 500-950 ºC [20-25]. Other compounds can also decompose at this temperature range and TGA is often coupled with a chemical analysis apparatus to identify the compounds being decomposed. FTIR also has a characteristic spectrum for the CO_3^{2-} ion in the wave number range of 1410-1510 cm^{-1} [80-30]. The TGA setup used did not have a chemical analysis unit so it was assumed that all mass loss in the appropriate temperature range was due to $CaCO_3$. If recarbonation had occurred in the sample then the weight loss in this temperature range should increase with respect to the increasing amount of $CaCO_3$ present. TGA was carried out both before and after testing to see the difference in the thermal decomposition of $CaCO_3$. An increase in mass lost in the specified temperature range after testing would correspond to more $CaCO_3$ being lost, so recarbonation had occurred.

All the samples exhibited much larger mass losses after testing in the temperature range of 500-950 ºC than before testing. The first differential curves with respect to temperature were also obtained for the samples as it allowed easy identification of the areas where the greatest mass loss had occurred and are shown in the figures below as the blue curve.

The TGA graphs showed that all the samples had undergone at least some recarbonation. Cement mortar samples were taken from each sample for testing. Every effort was made to collect a representative sample of the cement mortar from each sample, but this was not always possible. The <10 mm samples were mostly cement mortar powder and aggregate and this made retrieving a representative sample easy. The <40 mm sample proved more difficult as it had large particles and scraping a good mortar sample that was representative of the whole particle was difficult. Cement mortar samples were only taken from the exterior of the uncrushed samples to show that recarbonation had occurred in the sample, albeit at a very slow rate. Most of the samples exhibited a mass loss of 8-12% after CO_2 exposure. These values were a lot higher than before CO_2 exposure and show that much more of the mass present was now $CaCO_3$.

The smaller crushed sizes of <10 mm and <20 mm for both design mixes exhibited greater mass loss in the stated temperature range than the <40 mm and uncrushed samples. This also indicated that the smaller particle sizes had undergone more extensive recarbonation. A summary of the TGA data is contained in Table 3.6. From the data in Table 3.6 it is clear that the mass loss in the temperature range of 500-950 •C is much larger after CO_2 exposure than before and this can be attributed to the increase in the

$CaCO_3$ present in the cement mortar. The 20 MPa <10 mm and <20 mm samples also showed a larger mass loss before testing, which may indicate that some partial recarbonation may have occurred prior to testing. There is also a peak around the 350-400 °C mark in all the samples and this was responsible for the liberation of H_2O from $Ca(OH)_2$ [20-21].

Design Strength	Sample	Percent of Mass Lost Before CO2 Exposure	Percent of Mass Lost After CO2 Exposure	Difference %
20 MPa	<10 mm	5.4	13.0	7.60
	<20 mm	2	13.6	11.60
	<40 mm	1.8	10.6	8.80
	Uncrushed	2.9	12.6	9.70
40 MPa	<10 mm	0.65	11.4	10.75
	<20 mm	0.91	9.9	9.03
	<40 mm	1.5	11.3	9.80
	Uncrushed	8.8	14.9	6.10

Table 3.6 Summary of TGA data showing the percentage mass loss both before and after CO_2 exposure.

Without a chemical analysis unit the compounds being decomposed at the specified temperature range could not be verified. It was assumed that only the CO_2 absorption and the subsequent $CaCO_3$ formation were responsible for any increase in the thermal decomposition of the sample in the temperature range of 500-950 °C. The TGA graphs below (Figures 3.13-3.17) are some examples of what a typical TGA spectra looks like both before and after recarbonation testing. A complete set of TGA spectra and FTIR spectra for all the samples tested is contained in Appendix 2.

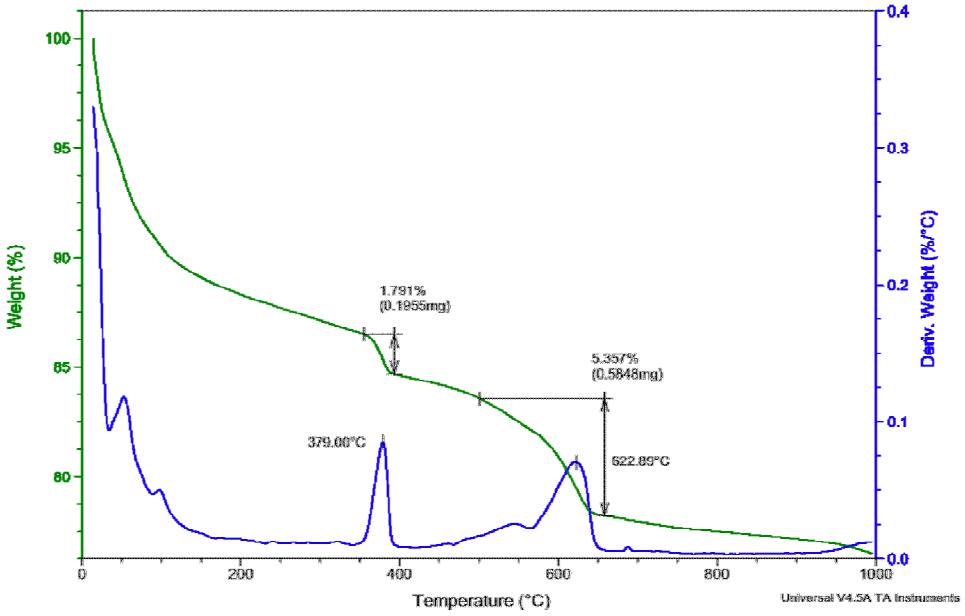

Figure 3.12 TGA spectrum of 20 MPa <10 mm sample before recarbonation testing. Note small peak at 500-700 ºC characteristic of CO_2 liberation.

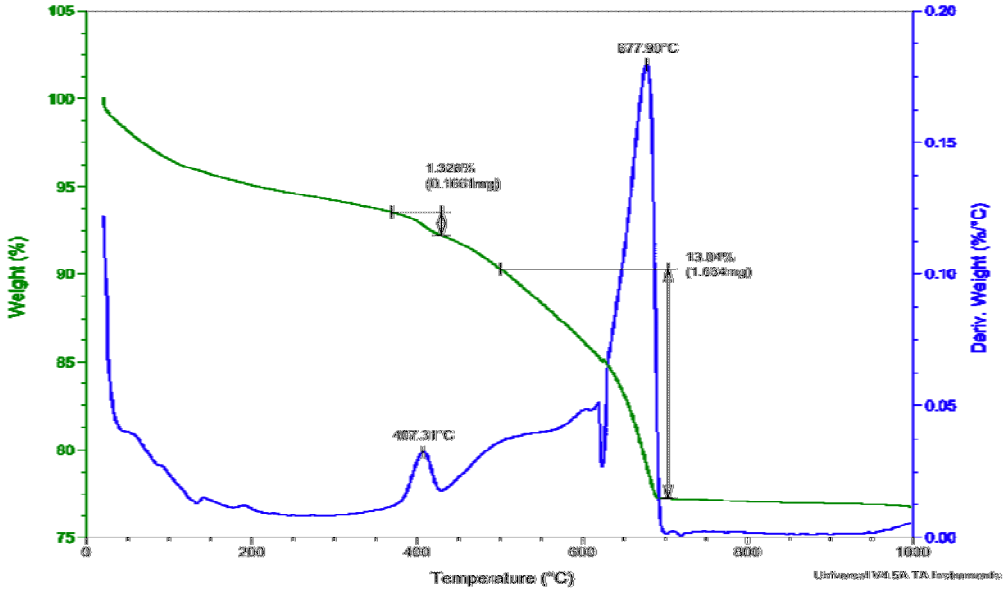

Figure 3.13 TGA spectrum of 20 MPa <10 mm sample before recarbonation testing. Note small peak at 500-700 ºC characteristic of CO_2 liberation.

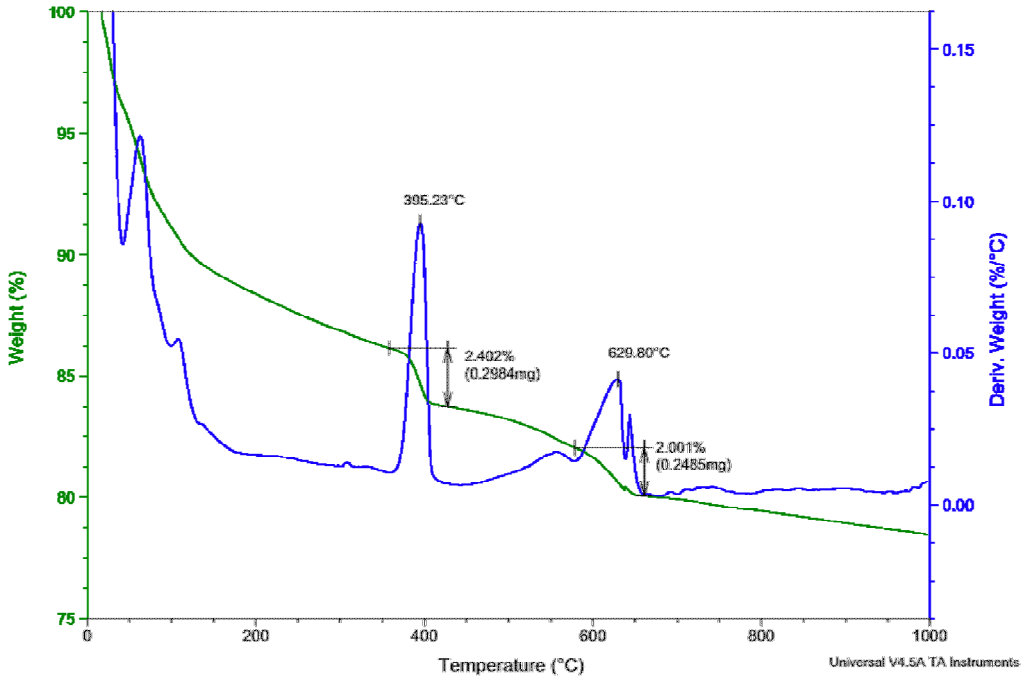

Figure 3.14 TGA spectrum of 20 MPa <10 mm sample before recarbonation testing. Note small peak at 500-700 ºC characteristic of CO_2 liberation.

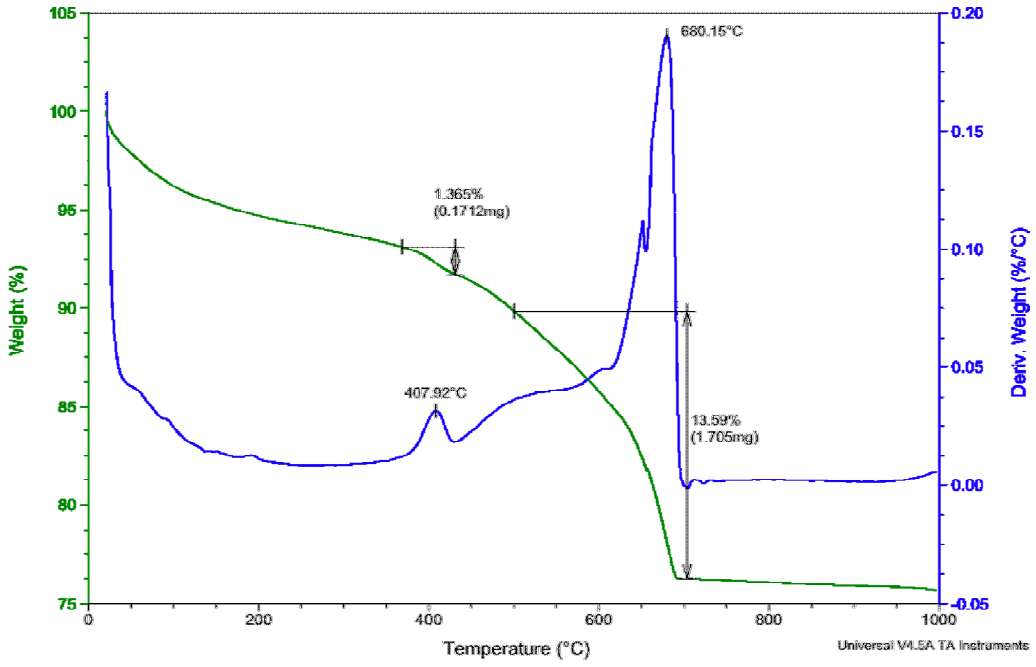

Figure 3.15 TGA spectrum of 20 MPa <10 mm sample before recarbonation testing. Note small peak at 500-700 ºC characteristic of CO_2 liberation.

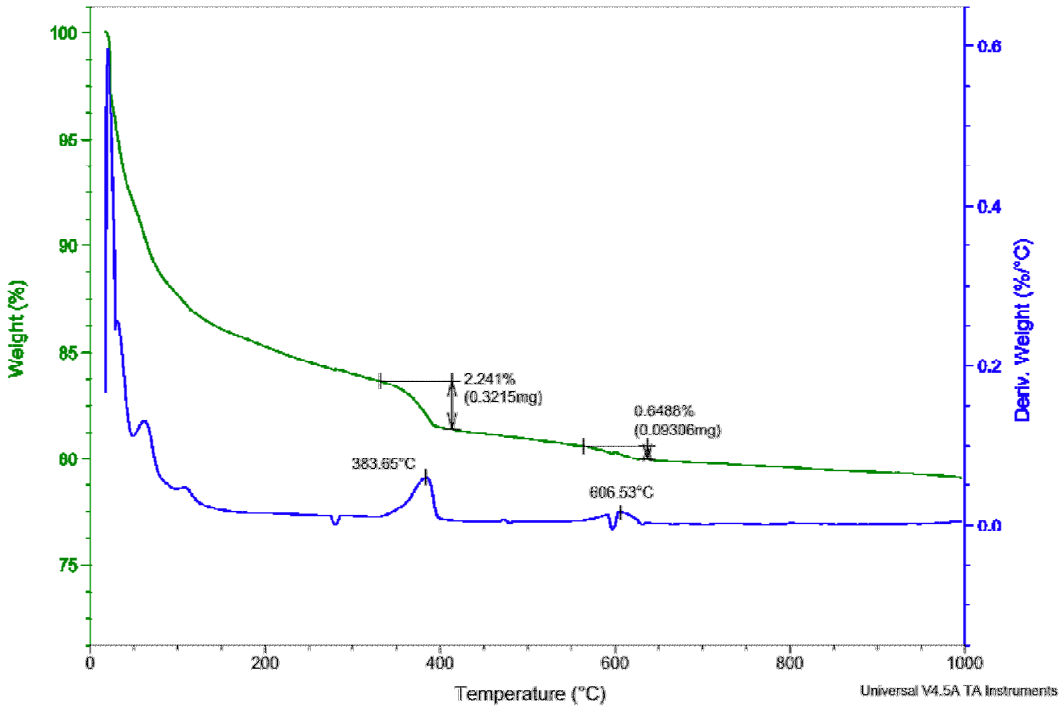

Figure 3.16 TGA spectrum of 20 MPa <10 mm sample before recarbonation testing. Note small peak at 500-700 ºC characteristic of CO_2 liberation.

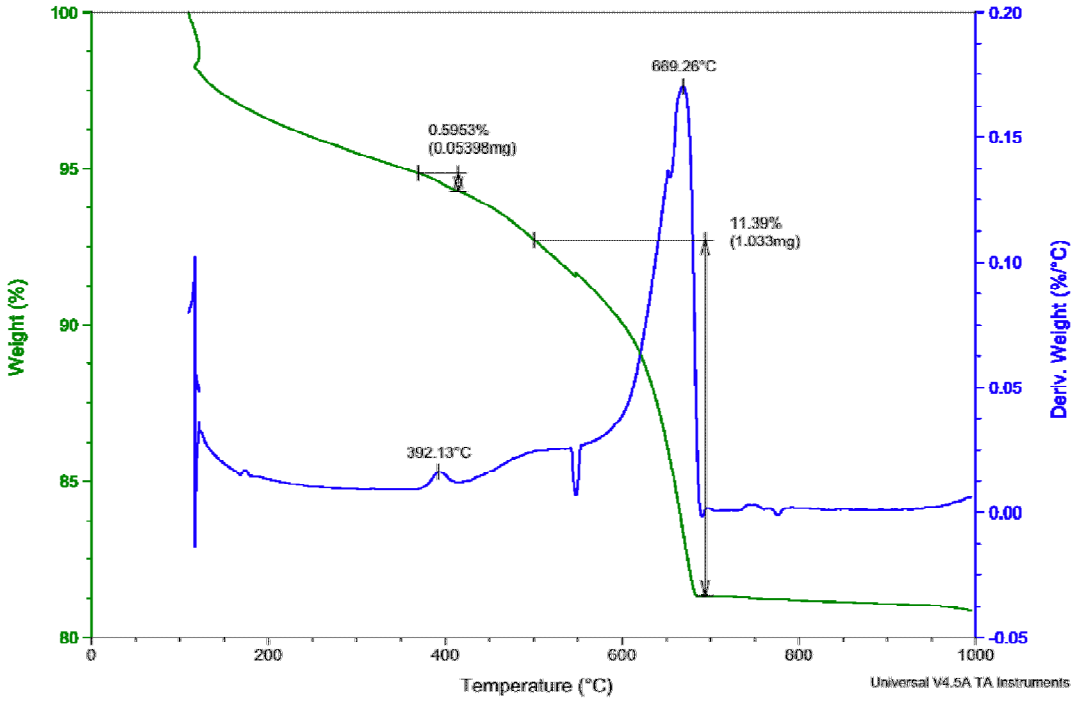

Figure 3.17 TGA spectrum of 20 MPa <10 mm sample before recarbonation testing. Note small peak at 500-700 ºC characteristic of CO_2 liberation.

The FTIR spectra were run in reflectance mode. It also quite likely that in this mode the spectrum was only probing the outer layers of the concrete particles and the resulting spectra may not be representative of the bulk. The FTIR spectra showed an increase of $CaCO_3$ present. As mentioned earlier the CO_3^{2-} ion exhibits a characteristic FTIR trough in the wave number range of 1410-1510 cm^{-1} [3,5,6,30]. The mortar samples taken after testing for FTIR analysis all showed an increase in the trough depth in the specified wave number range of 1410-1510 cm^{-1}. This would indicate that more $CaCO_3$ was present after CO_2 exposure than before. This confirms that recarbonation had taken place in the samples as more of the CO_3^{2-} ion was present. Figures 3.18-3.21 below show some typical FTIR spectra obtained for samples before and after CO_2 exposure. The FTIR spectra for all the samples are contained in Appendix 2.

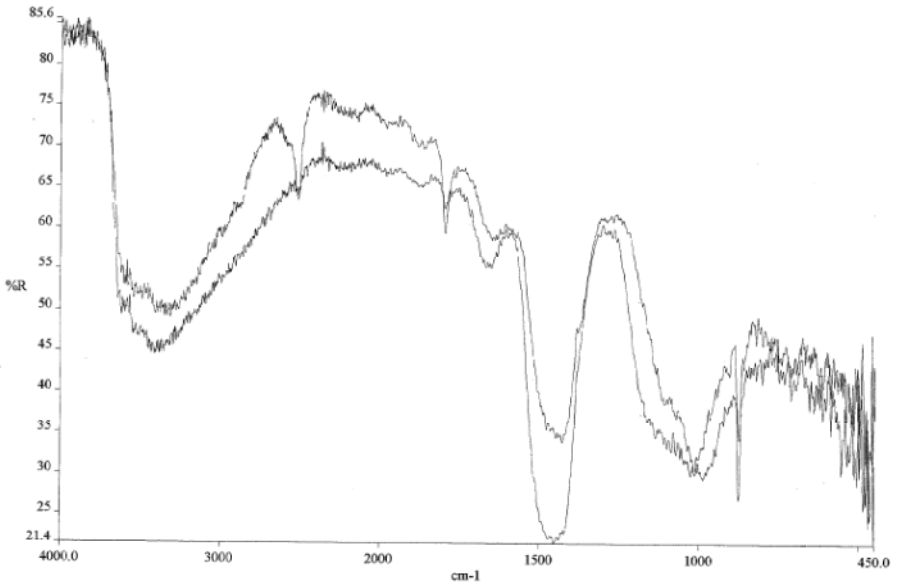

Figure 3.18 FTIR spectra of <10 mm 20 MPa sample. Note the increase in the trough depth at ~1500 cm^{-1}.

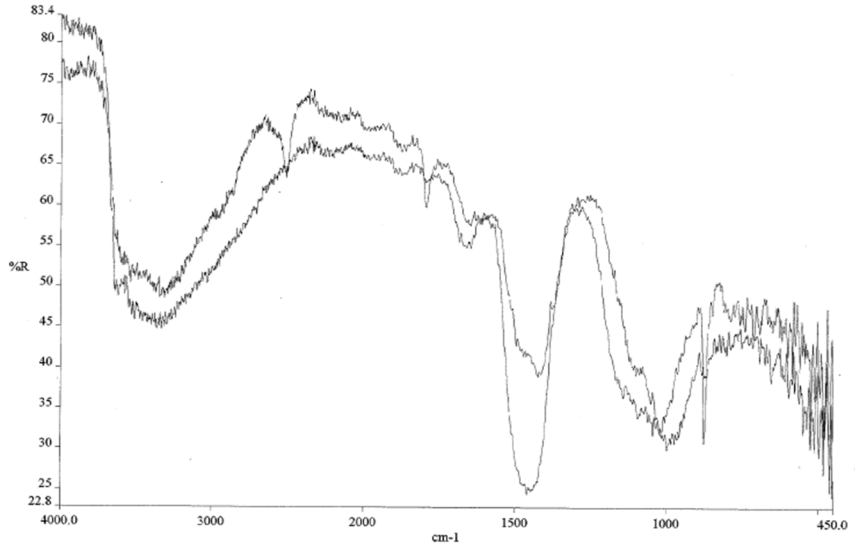

Figure 3.18 FTIR spectra of <10 mm 20 MPa sample. Note the increase in the trough depth at ~1500 cm^{-1}.

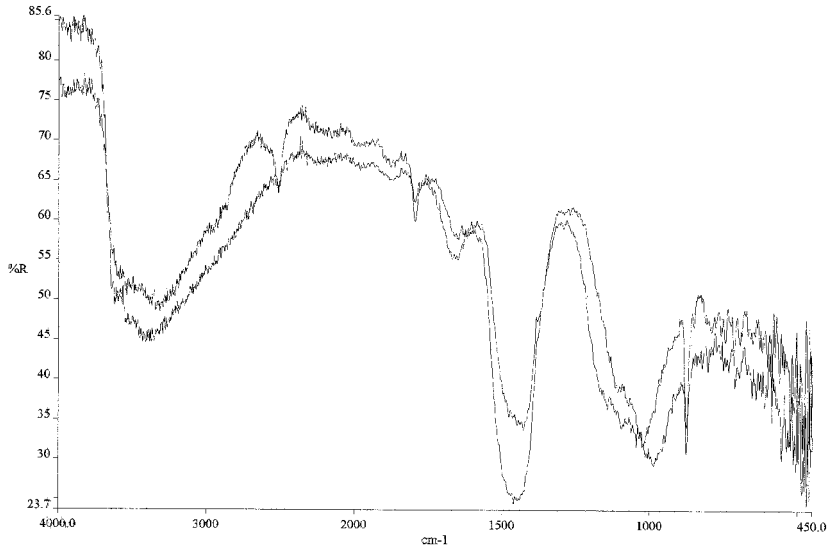

Figure 3.18 FTIR spectra of <10 mm 20 MPa sample. Note the increase in the trough depth at ~1500 cm^{-1}.

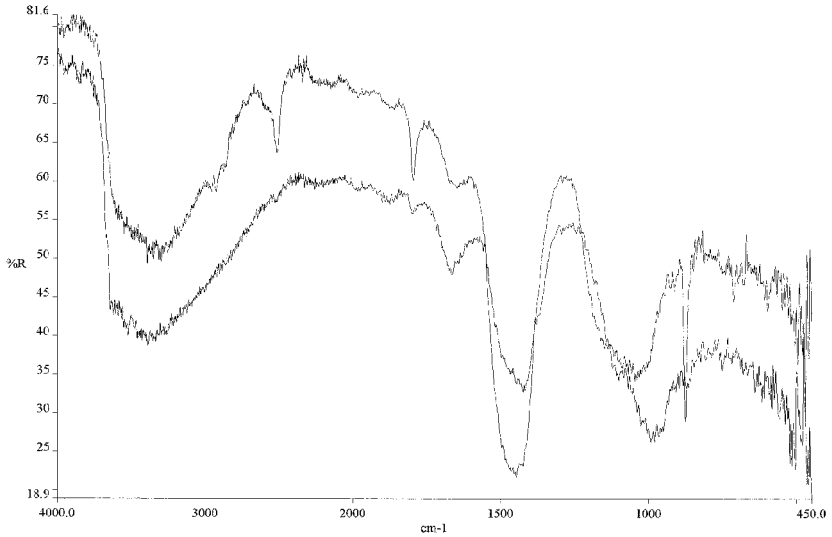

Figure 3.18 FTIR spectra of <10 mm 20 MPa sample. Note the increase in the trough depth at ~1500 cm^{-1}.

3.5.1 TGA and FTIR Summary

FTIR and TGA were used to confirm the infrared probe and weight gain results. FTIR and TGA were determined to be appropriate methods for detection of $CaCO_3$. Both methods showed an increase in the $CaCO_3$ concentration in the cement mortar after CO_2 exposure. For the TGA method it was assumed that all the mass lost in the temperature range of 500-950 °C was due to $CaCO_3$, as shown in previous studies [28-30]. FTIR also showed an increase in trough depth in the 1410-1510 cm^{-1} range after recarbonation testing that also corresponded to the presence of CO_3^{2-} [22-24].

The results from the TGA showed substantial thermal decomposition in the 500-950 °C temperature range after recarbonation testing for all the samples tested. For the 20 MPa design mix there was an average of 9.4% more mass lost in the specified temperature range after CO_2 exposure than before. The 40 MPa design mix showed similar results

with an average mass loss of 8.9% more after recarbonation testing than before recarbonation testing. These results verified the infrared probe results by showing that there had been an increase in the $CaCO_3$ concentration in the cement mortar for both 20 MPa and 40 MPa samples and that recarbonation had occurred. There was a problem with the TGA analysis though. The cement mortar samples were taken from the exterior of the samples that had been tested and were not representative of all the cement mortar present. This problem could have been solved using a chemical analysis unit coupled to the TGA. This would have enabled identification of the compounds being decomposed and their origin in the concrete matrix. Even without the attached chemical analysis unit the TGA curves were similar to those found in other studies [31-32].

The FTIR results also reinforced the results from the infrared probes and TGA. All the IR spectra demonstrated an increase in the reflectance in the wave number range 1410-1510 cm^{-1}. The trough generated in this wave number range by cement mortar has been shown to be attributable to CO_3^{2-} [30,32,34]. The increase in the trough depth for all cement mortar samples of both design strengths in this wave number range corresponds to the increase in CO_3^{2-} or $CaCO_3$, which is the main product of the recarbonation reaction.

3.6 Importance of this Research for the Cement and Concrete Industry

The manufacture of one tonne of cement is responsible for the release of 850 kg of CO_2 in New Zealand [7,8]. The intrinsic property of Ordinary Portland Cement to reabsorb some of these emissions once hydrated, has been the basis of this study. This is important for the cement and concrete industry as the net CO_2 emissions from cement over its life may be currently overestimated. This study looked at the recarbonation of crushed concrete and the extent of the reabsorption of the CO_2 emissions from the calcination of limestone. An accelerated recarbonation study using CO_2 specific infrared probes was used to measure the CO_2 uptake of crushed concrete with respect to particle size and cement composition in a controlled environment. This environment was 20 °C, relative humidity of 50-60 % and a maximum CO_2 concentration of 50,000 ppm (5%). Exposure of the samples occurred over a 21 day period.

The two design mixes used for testing were 20 MPa (w/c 0.67) and 40 MPa (w/c 0.49). Both design mixes were crushed to <10 mm, <20 mm and <40 mm particle sizes. Uncrushed sections of the concrete cylinders used were also tested to show that the recarbonation rate is drastically increased when the concrete is crushed. It was found that the 20 MPa design mix absorbed more CO_2 for all particle sizes than the 40 MPa design mix. Although the 40 MPa design mix had a greater cement content, the uptake was lower due to the decreased porosity of the concrete.

It was found that the 20 MPa design mix had a maximum uptake of 420 (g CO_2 / kg cement) for the <10 mm particle size and a minimum uptake of 60 (g CO_2 / kg cement) for the <40 mm sample in 21 days. The <20 mm sample for the 20 MPa design mix absorbed 360 (g CO_2 / kg cement) in 21 days. This corresponds to the reabsorption of 83, 72 and 12 % of the original calcinations emissions for the <10 mm, <20 mm and <40 mm particle sizes respectively. These results were in agreement with the Nordic Innovation Study [5] and the earlier statement that realistically 60-90 % of the CaO will undergo recarbonation depending on particle size and exposure conditions.

The 40 MPa design mix showed similar behaviour with the <10 mm particle size absorbing 350 (g CO_2 / kg cement) and the <20 mm sample absorbing 290 (g CO_2 / kg cement). For the 40 MPa design mix the <40 mm particle size had the lowest uptake of 47 (g CO_2 / kg cement). This corresponds to the reabsorption of 70, 57 and 9 % of the original calcinations emissions for the <10 mm, <20 mm and <40 mm particle sizes respectively. For both design mixes the uncrushed samples that were tested showed extremely low uptake rates (43 g CO_2 / kg cement for 20 MPa and 36 g CO_2 / kg cement for 40 MPa) when compared to the crushed concrete uptakes and reinforces engineers claims that uncrushed concrete carbonates very slowly.

From these results it is clear that the larger the surface area of the crushed concrete material, the greater the recarbonation rate. Particles with a size <10 mm seem to be very important for a rapid uptake. This can be confirmed by the particle size distributions in Figures 2.1 and 2.2. For both design mixes the <10 mm and <20 mm samples had large fractions of the 500 g samples below a particle size of 8 mm. These small particles aid rapid CO_2 uptake, as the <40 mm samples for both design strengths had a very small fraction that passed through the 8 mm sieve and hence their uptake was much lower.

These results are very important for the cement and concrete industry as the results indicate that some of the CO_2 released from the calcination of limestone during cement manufacture can be reabsorbed by the concrete. How much CO_2 that is reabsorbed is dependent on the particle size the concrete is crushed to, the cement content and the exposure conditions. A summary of the results with regard to CO_2 emissions of the cement during manufacture is shown in Table 3.7.

Design Strength	**Sample**	**Absorption (kg CO_2/tonne cement)**	**% Calcination Emissions Absorbed**	**CO_2 Emissions With Calcination Reductions (kg/tonne cement)**
20 MPa	<10 mm	420	83	430
	<20 mm	360	72	490
	<40 mm	60	12	790
	Uncrushed	43	9	807
40 MPa	<10 mm	350	70	500
	<20 mm	290	57	560
	<40 mm	47	9	803
	Uncrushed	36	7	814

Table 3.7 CO_2 uptakes of the crushed concrete samples showing the percentage of CaO recarbonated and the new emission figures for one tonne of cement with recarbonation reductions.

The original CO_2 emissions for one tonne of cement was 850 kg. From Table 3.7 it can be clearly seen that the <10 mm samples gave the biggest reduction of the total CO_2 emissions. From the original 850 kg of CO_2 emitted the <10 mm samples can absorb 420 (kg CO_2 /tonne cement) and 350 (kg CO_2 /tonne cement) for the 20 MPa and 40 MPa design mixes respectively. This means that 83 % and 70 % of the CaO present in the

cement mortar had undergone recarbonation. The extent of the CO_2 reductions for the <20 mm samples was not as great as the <10 mm samples but were still significant. These samples gave absorptions of 360 (kg CO_2 /tonne cement) and 290 (kg CO_2 /tonne cement) for the 20 MPa and 40 MPa design mixes respectively. This potentially reduced the total CO_2 emissions from the manufacture cement from 850 kg CO_2 to 490 kg and 560 kg, if a lifecycle approach is used for the crushed concrete material. This equates to 72 % and 57 % recarbonation of the CaO present in the cement mortar. The <40 mm particle size for both design strengths exhibited very low CO_2 uptakes in comparison to the <10 mm and <20 mm samples but was capable of reducing the original emissions to 790 (kg CO_2 /tonne cement) for the 20 MPa design mix and 803 (kg CO_2 /tonne cement) for the 40 MPa design mix. The uncrushed samples showed very little recarbonation activity and were good examples for demonstrating the increased CO_2 absorption rate when concrete is crushed.

It has been demonstrated that potentially up to 83 % of the original calcination CO_2 emissions can be absorbed by a 20 MPa design mix concrete when crushed to a particle size of <10 mm. This is almost half the original CO_2 emitted. The other particle sizes of <20 mm and <40 mm absorbed 72 % and 12 % of the calcination CO_2 emissions respectively. The samples with a 40 MPa design mix showed lower CO_2 uptake than that of 20 MPa and exhibited absorptions of 70, 57 and 9 % of the original calcination CO_2 emissions for particle sizes <10 mm, <20 mm and <40 mm.

The particle size and cement content are the most important factors in crushed concrete CO_2 absorption. When a crushed concrete sample contains particles with a diameter smaller than 8 mm the uptake rate appears to be very rapid. The larger the particle size becomes the smaller the surface area and the slower the recarbonation rate. The cement content is another determining factor in the recarbonation process. The more cement incorporated into the concrete the less porous the concrete matrix. The lower porosity means slower diffusion of the CO_2 into the concrete matrix. The other important factor for the recarbonation rate is the exposure conditions of the crushed concrete. This thesis used laboratory conditions with a temperature of 20±1.5 °C, a relative humidity of 50-60 % and CO_2 concentration of 50,000 ppm. As explained in detail in Section 1.5 it is not only the cement content and particle size that affect the recarbonation but the exposure conditions also.

In the context of the cement and concrete industry a 20 MPa (w/c 0.67) design mix has the potential to absorb 12-83 % of the original calcination CO_2 emissions when crushed to particle sizes of <40 mm, <20 mm and <10 mm respectively. The 40 MPa (w/c 0.49) design mix has the potential to reabsorb 9-70 % of the original calcination CO_2 emissions for the same particle sizes. This reduces net CO_2 emissions from cement manufacture by almost half if the concrete is crushed to <10 mm particle size. The larger particle sizes reabsorb some of the CO_2 emissions but not to the same extent as the <10 mm particle size. Therefore, of the original 850 kg of CO_2 emitted during the production of one tonne of cement, 47 – 420 kg can be reabsorbed by the concrete. This of course is dependent on cement content, crushed concrete particle size and exposure conditions. The <10 mm particle size demonstrated almost full recarbonation of all the CaO present in the cement in 21 days. This was achieved quickly as this was an accelerated recarbonation study. In the real world a <10 mm stockpile of concrete could potentially take 1-3 years to achieve the same result, at the atmospheric CO_2 concentration of ~0.038% and variable temperatures and humidities that the concrete would be exposed to.

The net CO_2 emissions for cement over its life are therefore currently overestimated, as they do not take into account the recarbonation potential of the concrete if it is crushed after its service life and stockpiled so that recarbonation can occur. For the recarbonation of concrete to be almost fully achieved and the majority of the calcinations CO_2 emissions reabsorbed, a particle size of <10 mm (for both design strengths) is most desirable as its CO_2 uptake is far greater than that of the particles sizes of <20 mm and <40 mm. Almost all the calcination CO_2 emissions can be reabsorbed if the concrete is crushed and exposed in ideal conditions and this can reduce the net CO_2 emissions from cement manufacture by almost half.

4.0 Conclusion

4.1 Key Results and Research Relevance

This thesis studied the recarbonation of crushed concrete in a New Zealand context. The thesis had three objectives:

1. Develop a test setup to measure the uptake of carbon dioxide by crushed concrete.
2. Determine how much carbon dioxide could be absorbed by crushed concrete and it potential for CO_2 reductions.
3. Determine how concrete composition and crushed concrete size affect the uptake of carbon dioxide by crushed concrete.

A test setup was developed to measure the recarbonation of crushed concrete using CO_2 specific infrared probes mounted in air tight desiccators. This method allowed control of the humidity, temperature and CO_2 concentration. The exposure conditions needed to be controlled to reduce the variables that could influence the recarbonation rate. The exposure conditions could be manipulated so that the maximum recarbonation rate could be achieved. This involved maintaining a relative humidity of 55-65 %, a temperature of 20 °C, a maximum CO_2 concentration of 50,000 ppm at one atmosphere pressure and an exposure period of 21 days. Other methods were also employed successfully to confirm the infrared probe results and were the weight gain of the samples, FTIR, TGA and phenolphthalein indicator.

There were many problems encountered in the construction of this setup as it had to be built from scratch. The setup eventually worked as planned but more refinements could be done to improve the operation and collection of data. Despite this the infrared probe setup provided a realistic measurement of the total CO_2 that was achievable for crushed concrete of varying particle sizes. It also provided quantification of the recarbonation rates for concrete of different cement contents. Other methods were employed successfully to confirm the infrared probe results and were the weight gain of the samples, FTIR, TGA and phenolphthalein indicator. The results were very similar to those found in the Nordic Innovation Centre study [10] of crushed concrete although different conditions and cements were used.

Crushed concrete of two different design mixes (20 MPa w/c 0.67 and 40 MPa w/c 0.49), made with OPC, have been shown to undergo recarbonation in this study. It was shown that crushed concrete will recarbonate at a much faster rate than uncrushed concrete. The largest CO_2 uptakes were observed for the <10 mm particle sizes of both design mixes. The <10 mm 20 MPa samples reabsorbed 420 (kg CO_2 / tonne cement) while the <10 mm 40 MPa sample reabsorbed 350 (kg CO_2 / tonne cement). This is the equivalent of 83 % and 70 % reabsorption of the calcination CO_2 emissions respectively. This would also indicate that the <10 mm samples were almost completely recarbonated in the 21 day period. The <20 mm samples also had significant CO_2 reabsorption. The <20 mm 20 MPa samples reabsorbed 360 (kg CO_2 / tonne cement) and the same particle size or the 40 MPa design mix reabsorbed 290 (kg CO_2 / tonne cement). This equated to 72 % and 57 % reabsorption of the calcination emissions.

The <40 mm particle sizes also demonstrated recarbonation behaviour but not to the same extent as the <10 mm and<20 mm samples. The 20 MPa <40 mm sample reabsorbed 60 (kg CO_2 / tonne cement) and the same particle size for the 40 MPa design mix reabsorbed 47 (kg CO_2 / tonne cement). In terms of CO_2 calcination emissions the 20 MPa sample reabsorbed 12 % and the 40 MPa sample reabsorbed 9 %.

The smaller particle sizes had a much faster uptake owing to their increased surface area for the same volume of crushed concrete material. The particles in the samples that were less than 10 mm in diameter appear to have the most influence on how quickly the CO_2 is absorbed. These results revealed that in order for rapid recarbonation to be achieved and a large amount of CO_2 to be reabsorbed, a particle size of at least <20 mm is desirable so long as a good proportion of the crushed material is less than 10 mm in diameter.

The cement content was also found to influence the recarbonation rate. Porosity is controlled by the water/cement ratio. A low water/cement ratio will decrease the porosity and a high water/cement ratio will increase the porosity [5,6,10]. As porosity increases, carbon dioxide diffusion increases resulting in an increased recarbonation rate. Concrete strength and density is inversely proportional to porosity. The denser the concrete becomes the slower the recarbonation rate as the concrete matrix becomes more confined. This was found to be true as the 40 MPa samples, even with a larger cement content, had lower recarbonation rates than that of the 20 MPa samples.

The total CO_2 released from the manufacture of cement in New Zealand is 850 kg [7,8]. Of this 850 kg approximately half is from the calcination of the limestone. This thesis has demonstrated recarbonation of crushed concrete of particle sizes <10, <20 and <40 mm for two different design strengths of 20 MPa and 40 MPa.

The maximum CO_2 uptake was observed for the <10 mm 20MPa sample which reabsorbed 420 (kg CO_2 / tonne cement). This equated to 83 % of the calcination emissions originally released and reduces the total CO_2 released from 850 kg to 430 (kg CO_2 / tonne cement). For the 40 MPa design mix the largest CO_2 uptake was also observed for the <10 mm sample. This had a CO_2 absorption of 350 (kg CO_2 / tonne cement) and accounted for 70% reabsorption of the original calcination emissions. This gave a reduction in the total original CO_2 emssions from 850 kg to 500 kg. The other crushed sizes also showed recarbonation behaviour but failed to achieve similar CO_2 uptakes as observed for the <10 mm samples.

This means that concrete with a w/c of 0.67 and 0.49 if allowed to recarbonate in a sufficient time frame, could reabsorb 70-83 % of the original calcination CO_2 emissions. This means that current estimates of the CO_2 released during cement manufacture are overestimated in the context of cements lifecycle as almost half the total CO_2 emitted in the manufacturing process can be reabsorbed if the concrete is crushed at the end of its useful life and allowed to recarbonate.

This research has shown that there is a significant opportunity to reduce CO_2 emissions from cement manufacture if a lifecycle approach is taken. With this in mind it is important for the cement and concrete industry to recognise the potential for recarbonation of crushed concrete and use this research to make a more informed decision on the impact of cement on the environmental over its lifetime.

4.2 Potential Improvements to Experimental Apparatus

The experimental setup involving the CO_2 specific infrared probes worked well as a recarbonation apparatus but there are improvements that could be made to the setup and sample preparation method.

The crushing of the concrete test cylinders was done in a compressive strength machine and screened for their appropriate particle size. Any particles that were unable to pass through the screen were recrushed manually so they could fit. This method was not representative of how concrete is crushed in the real world where commercial jaw crushers are used. The use of a variable jaw crusher was desirable but due to a lack of jaw crushers available with specifications required in Christchurch meant that the first method of crushing in a compressive strength machine was adopted. This allowed longer exposure of the crushed concrete samples to the atmosphere before testing than would have been the case for a variable jaw crusher. This meant that some recarbonation may have occurred in the samples prior to testing.

Another improvement that could be made involved the experimental setup. It was observed that the weight gains measured by the probes were not the same as that measured by weighing the samples before and after. This problem may have been solved by the running of a blank crushed sample that was not exposed to CO_2 and record any weight difference that occurred. This would mean that the weight change was not due to recarbonation but something else. As the testing began late, all the desiccators were needed for recarbonation testing and a blank was unable to be run.

Lastly the desiccators used were 2.5 L. This size desiccator was used because it was the only size available where six identical desiccators could be obtained. All the equipment and samples were able to fit into these but the conditions were cramped. Larger desiccators would be more desirable on a practical level as it would allow larger sample sizes to be tested and the conditions would not be so cramped.

4.3 Future Work

This thesis has only scraped the surface in terms of the research that can still be done into crushed concrete recarbonation. This study was limited to two concrete mix designs and had strict exposure conditions.

Future work in this area needs to address the recarbonation of other design strengths and effect of supplementary cementious materials such as blast furnace slag. This would give

a much more complete picture of recarbonation for a variety of cement types and allow greater understanding of the recarbonation potential of different design mixes.

As this study only looked at recarbonation of crushed concrete on a laboratory scale, real world tests need to be conducted for large crushed concrete stockpiles to see if the CO_2 uptakes obtained in the laboratory were reproducible in a real world context. Coupled to this could also be studies looking into the recarbonation rate using different exposure conditions. These conditions could be made to simulate a particular geographical area where a crushed concrete stockpile might be stored for recarbonation to occur. This would help to understand the areas and conditions needed for ideal recarbonation to occur in concrete stockpiles on a reasonable time scale. For instance a geographical area where it is cold will have a different period to achieve full recarbonation of the crushed concrete stockpile than an area where it is warmer.

The partial pressure of the CO_2 inside the desiccators was constantly changing as recarbonation occurred. This made the determination of any exact rate data hard as the kinetics of the recarbonation reaction always varied. Rate relationships could be achieved using a constant flow experiment. This would allow a constant CO_2 partial pressure to be achieved to study the reaction kinetics. This in turn would help to identify rate equations that could be used to estimate time periods and conditions needed for full recarbonation to occur.

5.0 References

[1] Crow, J.M., (2008), *The Concrete Conundrum*, Chemistry World, March 2008 (62-66).

[2] Sakai, K., (2009) *Towards Environmental Revolution in Concrete Technologies,* Environmental Concrete Seminar, September 2009.

[3] Claus, P., Guimaraes, M.; (2007); *The CO_2 uptake of concrete in a 100 year perspective*, Cement and Concrete Research, 37, (1348-1356).

[4] M.A. Peter, A. Muntean, S.A. Meir, M. Böhm; (2008); *Competition of several carbonation reactions in concrete: A parametric study*; Cement and Concrete Research, 38, (1385-1393).

[5] Taylor, H.F.W.; (1997); *Cement Chemistry*; Thomas Telford Publishing, 2nd ed.

[6] Lea, F.M.; (1970); *The Chemistry of Cement and Concrete,* Edward Arnold Publishing, 3rd ed.

[7] Holcim CO_2 Emission Data; Rynne, Michael; Holcim Cement (2008), Personal Communication.

[8] Len McSaveney, Golden Bay Cement (2008), Personal Communication.

[9] Halliday, L., Slaughter, G., Rynne, M., Totty, B.; (2006); *Ten Years of the New Zealand Used Oil Recovery Programme*, Holcim (New Zealand) Ltd, Internal Document.

[10] Christian J. Engelsen, Jacob Mehus, Claus Pade, Dag Henning Saether; (2005); *Carbon dioxide uptake in demolished and crushed concrete*, Nordic Innovation Centre Project 03018.

[11] Meir, S.A., Peter, M.A., Muntean, A., Böhm, M. ; (2006) ; *Dynamics of the internal reaction layer arising during carbonation of concrete,* Chemical Engineering Science, 62, (1125-1137).

[12] Houst, Y.F., Wittman, F.H. ; (2002) ; *Depth profiles of carbonates formed during natural carbonation,* Cement and Concrete Research, 32, (1923-1930).

[13] Johannesson, B., Utgenannt, P. ; (2001) ; *Microstructural changes caused by carbonation of cement mortar,* Cement and Concrete Research, 31, (925-931).

[14] Fernández Bertos, M., Simons, S.J.R., Hills, C.D., Carey, P.J.; (2004); *A review of accelerated carbonation technology in the treatment of cement-based materials and sequestration of CO_2*; Journal of Hazardous Materials, B112, (193-205).

[15] Sisomphon, K., Franke, L.; (2007); *Carbonation rates of concretes containing high volume of pozzolanic materials,* Cement and Concrete Research, 37, (1647-1653).

[16] Parrott, L.J.; (1987); *A review of carbonation in reinforced concrete,* A review carried out C&CA under a BRE contract, July 1987.

[17] Clear, C.A., De Saulles, T.; (2007); *BCA Recarbonation Scoping Study,* BCA Report, Version 2.2, June 2007.

[18] Pommer, K., Pade, C.; (2005); *Guidelines – Uptake of carbon dioxide in the life cycle inventory of concrete,* Nordic Innovation Centre Project 03018, Danish Technological Institute, October 2005.

[19] Gajda, J., MacGregor Miller, F.; (2000); *Concrete as a Sink for Atmospheric carbon Dioxide: A Literature Review and Estimation of CO_2 Absorption by Portland Cement Concrete,* R&D Serial No. 2255, Portland Cement Association, 2000.

[20] Loo, Y.H., Chin, M.S., Tam, C.T., Ong, K.C.G.; (1994); *A Carbonation Prediction Model for Accelerated carbonation testing of Concrete,* Magazine of Concrete Research, 46, No. 168, September, (191-200).

[21] Dinku, A., Reinhardt, H.W.; (1996); *the influence of Storage Conditions on the Gas Permeability and carbonation of Concrete,* Concrete repair, rehabilitation and Protection.

[22] Ogawa, Y., Kaji, T., Shima, H., Nakamura, H.; (1995); *Compressive Strength and Pore Volume of No-Fines Porous Concrete Absorbing carbon Dioxide Gas,* Transactions of the Japan Concrete Institute, Vol. 17, (53-60)

[23] Papadakis, V.G., Vayenas, C.G., Fardis, M.N.; (1989); *A reaction engineering approach to the problem of concrete carbonation*; Journal of Applied Chemical Engineering, Vol. 35, No. 10, (1639-1650).

[24] Chen, J.J., Thomas, J.J., Taylor, H.F.W., Jennings, H.M.; (2004); *Solubility and structure of calcium silicate hydrate*; Cement and Concrete Research, 34, (1499-1519).

[25] Jerga, J.; (2004); *Physico-mechanical properties of carbonated concrete,* Construction and Building Materials, 18, (645-652).

[26] Ati• C.D.; (2003); *Accelerated carbonation and testing of concrete made with fly ash,* Construction and Building Materials, 17, (147-152).

[27] Roy, S.K., Poh, K.B., Northwood, D.O.; (1999); *Durability of concrete – accelerated carbonation and weathering studies*; Building and Environment, 34, (597-606).

[28] Menadi, B., Kenai, S., Khatib, J., Aït-Mokhtar, A.; (2009); *Strength and durability of concrete incorporating crushed limestone sand,* Construction and Building Materials, 23, (625-633).

[29] Hui-sheng, S., Bi-wan. X., Xiao-chen, Z.; (2008); *Influence of mineral admixtures on compressive strength, gas permeability and carbonation of high performance concrete,* Construction and Building Materials, Article in Press, doi:10.1016/j.conbuildmat.2008..08.021.

[30] Jiang, L., Lin, B., Cai, Y.; (2000); *A model for predicting carbonation of high volume fly ash concrete,* Cement and Concrete Research, 30, (699-702).

[31] Castellote, M., Andrade, C., Turrillas, X., Campo, J., Cuello, G.J.; (2008); *Accelerated carbonation of cement pastes in situ monitored by neutron diffraction,* Cement and Concrete Research, 38, (1365-1373).

[32] Lo, Y., Lee, H.M.; (2001); *Curing effects on carbonation of concrete using a phenolphthalein indicator and Fourier-transform infrared spectroscopy,* Building and Environment, 37, (507-514).

[33] Villian, G., Thiery, M., Platret, G.; (2007); *Measurement methods of carbonation profiles in concrete: Thermogravimetry, chemical analysis and gammadensimetry*; Cement and Concrete Research, 37, (1182-1192).

[34] Chang, C., Chen, J.; (2006); *The experimental investigation of concrete carbonation depth*, Cement and Concrete Research, 36, (1760-1767).

[35] Nikulshina, V., Gálvez, M.E., Steinfeld, A.; (2007); *Kinetic analysis of the carbonation reactions for the capture of CO_2 from air via the $Ca(OH)_2$-$CaCO_3$-CaO solar thermochemical cycle,* Chemical Engineering Journal, 129, (75-83).

[36] Tam, V.W.Y., Gao, X.F., Tam, C.M.; (2005); *Carbonation around near aggregate regions of old hardened concrete cement paste,* Cement and Concrete Research, 35, (1180-1186).

[37] Levy, S.M., Helene, P.; (2004); *Durability of recycled aggregates concrete: a safe way to sustainable development,* Cement and Concrete Research, 34, (1975-1980).

[38] Li, X.; (2008); *Recycling and reuse of waste concrete in China Part I. Material behaviour of recycled aggregate concrete,* Resources, Conservation and Recycling, Article in Press, doi:10.1016/j.resconrec.2008.09.006.

[39] New Zealand Standard 3112-1986, New Zealand Qualifications Authority, 2008, Version 5.

[40] Huntzinger, D.; (2006); *Carbon Dioxide Sequestration in Cement Kiln Dust Through Mineral Carbonation,* Dissertation, Michigan Technological Institute.

6.0 Appendix 1 and 2

The CD-ROM attached to this thesis contains electronic versions of the LabView circuit diagram, TGA spectra and FTIR spectra. There are three folders that contain these files. There is also a PDF version of the entire thesis in the folder ‘Thesis’ should the reader require an electronic copy. (PDF files can be viewed in the Adobe Acrobat Reader program, which available as a free download from the Adobe website www.adobe.com/products/acrobat/readermain.html)

The LabView folder contains PDF files of the circuit diagram and programming operations and an overview of the front panel used to control the experiment and are labelled accordingly.

The TGA spectra are contained in the folder ‘TGA Spectra’ and are in PDF format. The names of the files correspond to the sample spectra contained within of which some were shown in the thesis.

The FTIR spectra are also in PDF format contained in the folder ‘FTIR Spectra’. The names of the files represent the spectra contained within. Each file has two spectra for all the samples showing before and after recarbonation testing.